

## Article

# Intraplate Strike-Slip Corridor within South America (NE Border of the Paraná Basin) Unveiled by Structural Analysis of Faults and Fracture Swarms

Paola Cianfarra <sup>1,\*</sup>, Marcos Roberto Pinheiro <sup>2</sup>, Fernando Nadal Junqueira Villela <sup>2</sup> and Francesco Salvini <sup>3</sup>

<sup>1</sup> Dipartimento di Scienze della Terra, dell'Ambiente e della Vita, Università degli Studi di Genova, I-16132 Genova, Italy

<sup>2</sup> Laboratory of Pedology, Department of Geography, Faculty of Philosophy, Languages and Human Sciences, University of São Paulo, São Paulo 05508-000, SP, Brazil; m3279574@usp.br (M.R.P.); geovillela@usp.br (F.N.J.V.)

<sup>3</sup> GeoQuTe Lab, Università degli Studi Roma Tre, I-00146 Roma, Italy; francesco.salvini@uniroma3.it

\* Correspondence: paola.cianfarra@unige.it; Tel.: +39-347-0625674

**Abstract:** We present the effect of neotectonics in intracratonic settings as revealed by the surface, brittle deformation associated to a regionally-sized shear corridor, which affects Southeastern Brazil. The deformation zone is characterized by the presence of nearly orthogonal fracture sets, interpreted as systematic and non-systematic joints often cutting Quaternary deposits. An original methodology of fault and joint inversion by the Monte Carlo converging approach is used to infer multiple paleostress fields. The method provides the best orientation of the principal paleo-stresses responsible for the observed fracturing. At each step of the inversion process, structures are uniquely associated to the stress tensor that provides the lowest error. The results showed the poly-phased tectonic history of the shear corridor studied and paleostresses compatible with a regional strike-slip motion. Specifically, an E-W, left-lateral shear was followed by an E-W, right-lateral kinematics related to the post-Paleogene drifting of South American Plate and its clockwise rotation. The latter tectonic event is presently responsible for brittle deformation observed in Quaternary deposits. The proposed deformation corridor may represent the Cenozoic reactivation of an ancient weakness zone. We speculate that the described intraplate strike-slip deformation belt represents the continental prosecution of the Rio de Janeiro fracture zone.

**Keywords:** intraplate tectonics; neotectonics; reactivation of inherited weakness zones; multiple paleostresses; Monte Carlo direct inversion



**Citation:** Cianfarra, P.; Pinheiro, M.R.; Villela, F.N.J.; Salvini, F. Intraplate Strike-Slip Corridor within South America (NE Border of the Paraná Basin) Unveiled by Structural Analysis of Faults and Fracture Swarms. *Geosciences* **2022**, *12*, 101. <https://doi.org/10.3390/geosciences12020101>

Academic Editors: Ian Alsop and Jesus Martinez-Frias

Received: 30 November 2021

Accepted: 16 February 2022

Published: 21 February 2022

**Publisher's Note:** MDPI stays neutral with regard to jurisdictional claims in published maps and institutional affiliations.



**Copyright:** © 2022 by the authors. Licensee MDPI, Basel, Switzerland. This article is an open access article distributed under the terms and conditions of the Creative Commons Attribution (CC BY) license (<https://creativecommons.org/licenses/by/4.0/>).

## 1. Introduction

The classical paradigm of plate tectonic theory assumes that deformation associated to plate interactions is concentrated into narrow belts along the plate margins and that the lithosphere in the plate interiors is, to a first approximation, rigid and relatively stable (Morgan [1]; Holdsworth et al. [2]; Wilson et al. [3]). This is true for regions underlain by oceanic lithosphere. On the other hand, the non-rigid behavior of continental lithosphere is widely acknowledged (Holdsworth et al. [2]; Storti et al. [4]) and relates also to the presence of pre-existing anisotropies locked into the continents and associated to old faults and shear zones that can experience reactivation during successive phases of regional deformation episodes (Dewey et al. [5]; Molnar [6]). The presence and reactivation of inherited crustal weakness corridors strongly influence the formation of intracratonic basins, the location and architecture of the continental breakup, post-rift spreading and offshore fracture zones propagation (Dewey et al. [5]; Daly et al. [7]; Hasui [8]; Vasconcelos et al. [9]). The Paraná Basin (Figure 1), among the five largest Phanerozoic basins of the South American platform, with its intracratonic setting and long lived tectonic history, represents a key site to study

processes associated to the reactivation of intraplate inherited weakness shear zones and orogenic sutures.

The geological history of the Paraná Basin and its surroundings was influenced by the geodynamics of the western Gondwana, a structural domain that suffered during almost all the Phanerozoic eon poly-phased tectonics associated to the reactivation of Proterozoic mobile belts (e.g., Zalán et al. [10]; Almeida et al. [11]; Vaughan and Pankhurst [12]). The reactivation of inherited crustal weakness shear zones relates to the intraplate response of the late, Paleozoic stages of Pangea amalgamation followed by its Mesozoic breakup, post-rift spreading and drifting (Torsvik et al. [13]; Hasui [8]).

The current geodynamic setting of South American intracratonic regions is characterized by the ongoing South Atlantic opening, the clockwise rotation of South America and the convergence between South America and Nazca plates (Lima et al. [14]). The development of new, intraplate shear zones that ease/accomplish the regional kinematics together with the reactivation of inherited crustal structures is an open issue (e.g., Roberts and Holdsworth [15]; Bezerra et al. [16]; Vasconcelos et al. [9]). The vast majority of the scientific production mainly concerns with the Proterozoic, Paleozoic and Mesozoic history of the main tectonic trends within South America (e.g., Fulfaro et al. [17]; Soares et al. [18]; Unternehr et al. [19]; Zalán et al., [20]; Eyles et al. [21]), especially in the Brazilian territory. The role of Neotectonics (e.g., the current tectonic regime active since the Miocene; Hasui [8]) is still a matter of debate. Nevertheless, the presence in the last hundreds of years of medium-to-low energy seismicity (moment magnitude up to 4.5) in intraplate settings strongly suggests the role of active tectonics. Most researches performed on the neotectonics of South America are published in Portuguese language journals or still remain unpublished. The present paper aims to contribute in filling this gap and to better understand the neotectonics in the intraplate Brazilian territory, with a special focus in the northeastern border of the Paraná Basin. This in turn will allow mitigation of the hydrogeologic risk in the study area where many hydroelectric power plants are located.

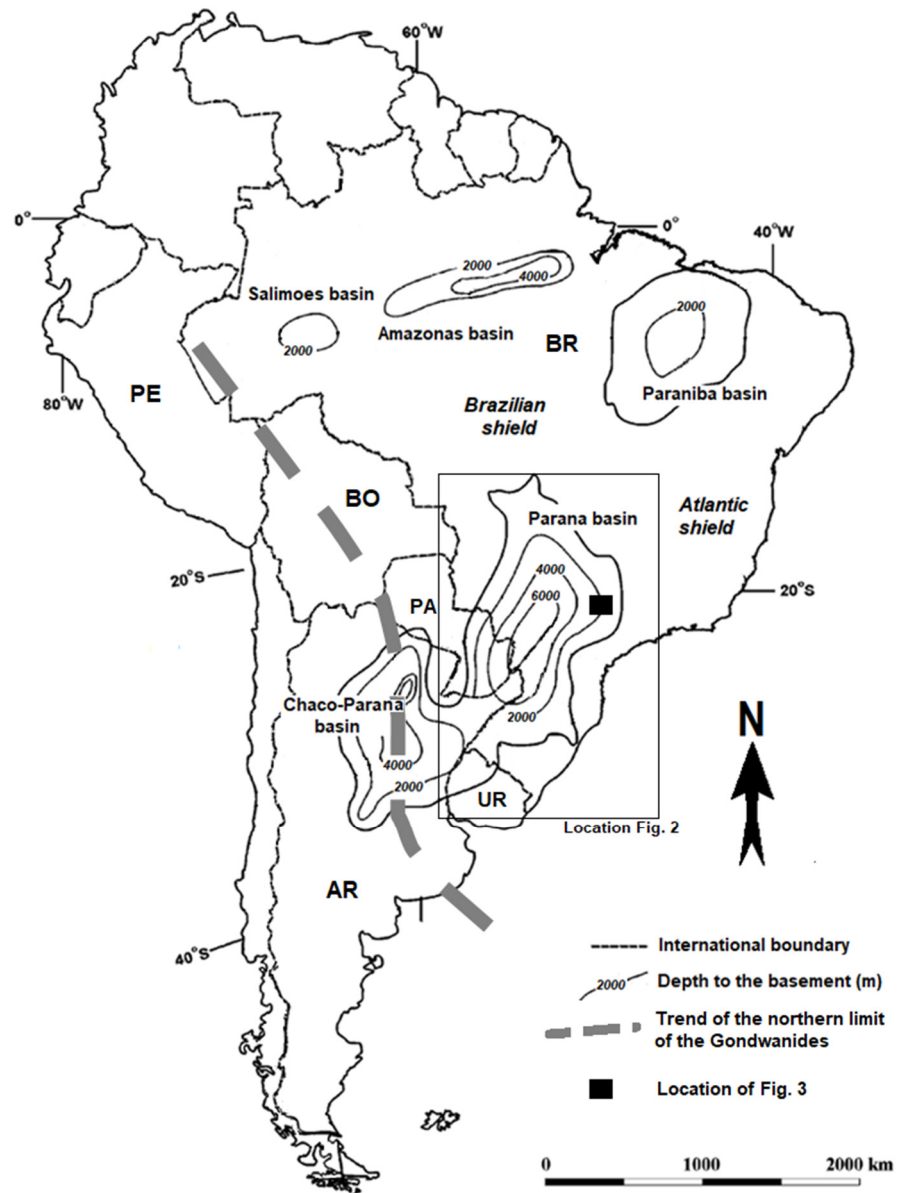


**Figure 1.** The five main intracratonic basins within South America: Solimões, Amazonas, Parnaíba, Paraná and Chaco-Paraná Basin (Milani et al. [22]). AR: Argentina; BO: Bolivia; BR: Brazil; PA: Paraguay; PE: Peru; UR: Uruguay.

## 2. Geodynamic and Regional Tectonic Setting

The general framework of the Brazilian shield is made of a few Archean and Paleoproterozoic cratonic nuclei surrounded by Pan-African–Brazilian mobile belts of Neoproterozoic age (Almeida [23]; Brito Neves and Cordani [24]; Almeida et al. [11]; Campanha and Brito Neves [25]). The relics of significant Paleozoic sedimentation all over the South American continent are preserved in five basins (Figure 1; Milani and Zalán [26]). Solimões, Amazonas, Parnaíba and Paraná, named after large rivers that flow along their main axes, are located in the Brazilian territories; the Argentinian Chaco-Paraná Basin is included in the wide sub-Andean flat area that spans all the western portion of the continent. These basins are characterized by an overall elliptical to semi-circular geometry and are surrounded by exposures of Precambrian shields.

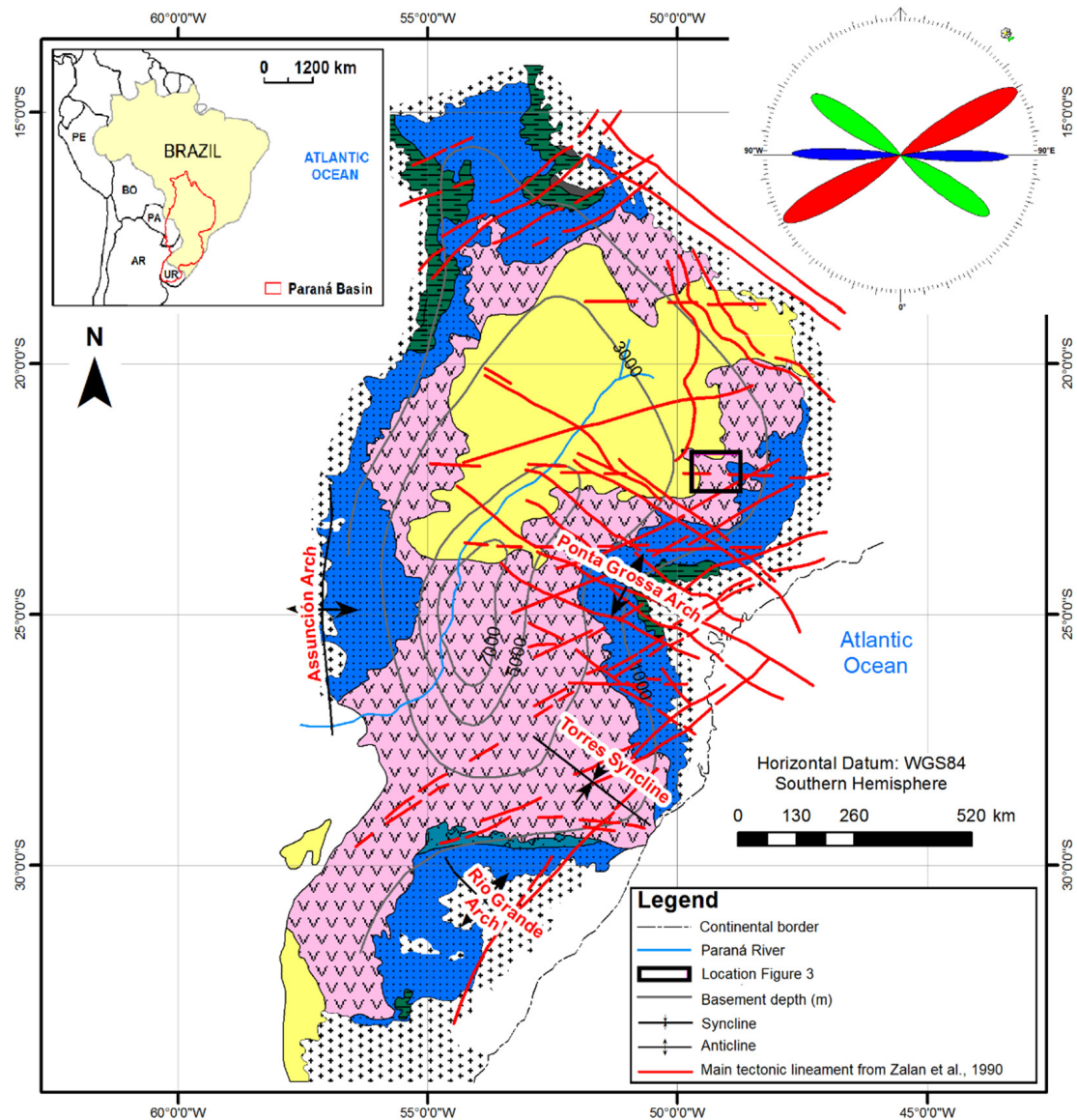
These intracratonic depressions were largely filled with siliciclastic sedimentary deposits testifying large-scale Paleozoic transgressive–regressive cycles (Milani et al. [22]). The only exception is represented by the evaporite–carbonate cycle in the Solimões and Amazonas. In most basins, the first cycles usually show marked glacial influences with ages that vary between the late Ordovician (Paraná) and the Devonian (Solimões and Amazonas), depending on the location of the basins over the Gondwana supercontinent that has been wandering around the south polar regions (Caputo and Crowell [27]). In the case of the Paraná and Chaco-Paraná Basins, this glacial influence reappeared strongly in the Late Carboniferous, during the inception of the third transgressive–regressive cycle. In all the five basins, the last transgressive–regressive cycle is almost uniformly sutured by late Permian to Triassic continental red beds that mark the drying out of the interior sags and the definitive disappearance of the seas from the cratonic areas of South America. The Mesozoic history of these basins is recorded as continental sedimentary packages and large volumes of magmatic rocks (Riccomini et al. [28]). The rifting of Western Gondwana and opening of South Atlantic during Early Cretaceous (Renne et al. [29]) was associated with the Paraná-Etendeka large igneous province (Peate [30], Gomes and Vasconcelos [31]; Rossetti et al. [32]). The volcanic pile is characterized by tholeiitic basalts and basaltic andesites which span a broad geochemical spectrum. Giant dyke swarm, intrusive complexes and volcanic centers occur associated with the main flood lavas and are well preserved in both South American and African coasts (Peate [30], Richetti et al. [33]). The Paraná-Etendeka lavas were deposited over and are intercalated with aeolian sandstones (Botucatu-Tweifelfountain Group, Rossetti et al. [34]). In Brazil, continental flood basalts and silicic rocks fall within the Serra Geral Formation in the Paraná Basin (Rossetti et al. [34]). In the African counterpart, the Paraná-Etendeka lavas include the Etendeka Group in Namibia (Erlank et al. [35]) and the Cretaceous volcanic rocks of the Kwanza basin in Angola (Marzoli et al. [36]).

### 2.1. The Paraná Basin

The intracratonic Paraná Basin is a vast geotectonic province of South America located in southern Brazil spanning through four countries, namely Brazil, Argentina, Paraguay and Uruguay, with an area of about 1.4 million of square km (Figures 1 and 2).

The basin has a NNE-SSW trending elliptical shape with two-thirds of its surface covered by Mesozoic basaltic lavas. The infilling sedimentary package crops out along 5.500 km belt shaped during Mesozoic-Cenozoic times. The stratigraphic record of the basin exceeds 7000 m thickness in the central depocenter and ranges from Upper Ordovician to Upper Cretaceous time (Milani [37]). The Precambrian basement of the Paraná Basin has a complex crustal framework (Soares et al. [38]; Cordani et al. [39]; Zalán et al. [10]; Soares [40]; Almeida et al. [11]), consisting of granite-gneissic terranes (Zalán et al. [10]) surrounded by fold and thrust belts (Cordani et al. [39]) formed during the end of the Neoproterozoic and Early Paleozoic times (Almeida and Hasui [41]; Almeida and Melo [42]; Almeida et al. [11]; Zalán et al. [10]; Milani and Ramos [43]).

The eastern flank of the Paraná Basin includes a crustal region affected by the South Atlantic rifting and following drifting. These events produced the uplift of the Atlantic region of the Southeastern Brazil (Tello Saenz et al. [44], Ribeiro et al. [45], Godoy et al. [46]) and subsequent erosion responsible for the removal of great amounts of Paleozoic sedimentary covers from that area (Pinheiro & Queiroz Neto [47]). In the western border of the basin is present the Asunción arch, a flexural bulge related to the loading of the Cenozoic Andean thrust sheets in nearby Argentina and Bolivia (Riccomini et al. [28]). To the north and to the south, the Paraná Basin sedimentary cover onlaps the Precambrian crystalline rocks of basement (Milani et al. [22]).



**Supersequences**

- Bauru (Upper Cretaceous): very fine to coarse sandstones (eventually with calcium nodules), siltstones and shales.
- Gondwana III (Late Jurassic to Eo-Cretaceous): fine to coarse sandstones and basalt flows.
- Gondwana II (Triassic): fine to coarse sandstones, conglomerates, siltstones and pelites
- Gondwana I (Upper Carboniferous to Eo-Triassic): tillites, diamictites, varves, sandstones, siltstones, shales and coals.
- Paraná (Devonian): fine to coarse sandstones, siltstones and mudstones.
- Rio Ivai (Upper Ordovician to Eo-Silurian): sandstones, diamictites, shales, siltstones and basalts.
- Proterozoic Basement

**Figure 2.** Simplified geologic-structural map of the Paraná Basin. Rose diagram (upper right) of the fault azimuthal frequency shows the three main structural trends (fault and fault zones with ages ranging from Paleozoic to Mesozoic, Zalán et al. [20]) of the region, namely NW-SE, NE-SW and E-W. AR: Argentina; BO: Bolivia; BR: Brazil; PA: Paraguay; PE: Peru; UR: Uruguay. (Modified from Zalán et al. [20]).

The Late Ordovician inception and further evolution of the Paraná Basin in the continental interior of west Gondwana is related to the development of the Gondwanides, a large Phanerozoic mobile belt that suffered a series of orogenic cycles (Milani and Ramos

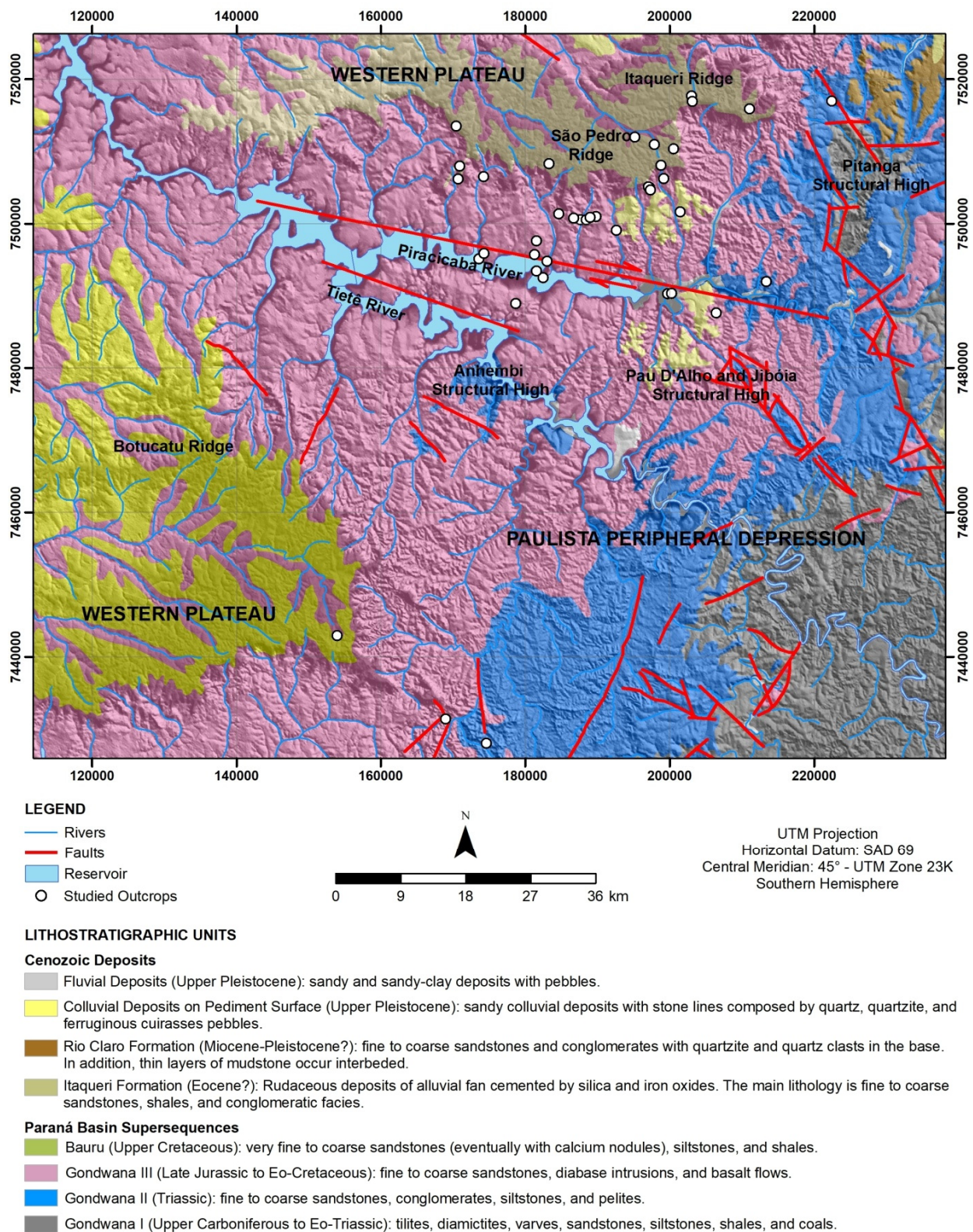
43). These basement weakness zones exerted a decisive influence on the creation of accommodation space for the supersequences filling the Paraná Basin (Milani [37]; Milani and Ramos [43]), as well as on the deformational history of the basin (Zalán et al. [20]), by means of intraplate reactivation of NE-SW-trending inherited crustal weakness zones and cratonward propagation of regional flexural subsidence (Milani and Zalán [26]).

The stratigraphic record of the Paraná Basin consists of six supersequences (Milani [37], Figures 2 and 3): Rio Ivaí (Caradoc-Llandovery/Ordovician-Silurian), Paraná (Lockvian-Frasnian/Devonian), Gondwana I (Westphalian-Scythian/Carboniferous-Lower Triassic), Gondwana II (Anisian-Norian/Middle to Upper Triassic), Gondwana III (Upper Jurassic-Berriasian/Upper Jurassic-Lower Cretaceous) and Bauru (Aptian-Maastrichtian/Upper Cretaceous). Three of them correspond to Paleozoic transgressive–regressive cycles, and the others are Mesozoic continental sedimentary packages with associated igneous rocks. These igneous rocks are related to the Gondwana supercontinent rupture (200 Ma), which resulted in the opening of the Atlantic Ocean, at about 120 Ma (Mizusaki & Thomaz-Filho [48]). This major geodynamic episode was registered in the Paraná Basin during the Early Cretaceous as magmatism (e.g., Paraná-Etendeka large igneous province, Peate [49]; Renne et al. [29]) with tholeiitic and calc-alkaline basalts, and subordinate rhyolites and rhyodacites, which characterize the Serra Geral Formation (Peate et al. [49]; Riccomini et al. [28]). The breakup of Gondwana and South Atlantic opening are possibly linked to a large plume impacting the supercontinent (e.g., Bryan et al. [50]).

The initial subsidence in the basin and the marine transgression, related to the reactivation of NE-SW basement structures (Milani et al. [22]; Zalán et al. [20]), lasted from Ordovician until mid-Devonian and was followed by the Frasnian regression. According to Almeida [51] and Milani [37], the tectonic and sedimentary history of the Paraná Basin can be divided into four phases. From Carboniferous to Middle Permian there was an intense tectonic activity with the deposition of sediments (Tubarão Super group—Gondwana I Supersequence) under prevailing glacial conditions. Successively, a weak tectonic activity lasted until the Upper Permian and led to the slow subsidence of the central Paraná Basin. At the end of the glacial period there was a renewed marine transgression with the deposition of the Passa Dois Group (Gondwana I Supersequence) in deep-to-shallow marine and fluvial/lacustrine/tidal environments.

From Triassic to Eo-Cretaceous times, there was a weak tectonic activity associated to local slow subsidence and deposition of the aeolian and fluvial sediments of the Botucatu and Piramboia Formations (São Bento Group—Gondwana II and III Supersequences) under desert conditions. The successive opening of the South Atlantic with massive volcanic eruptions (Serra Geral Formation—Gondwana III Supersequence) in Eo-Cretaceous time was associated with the reactivation of old tectonic structures and the deposition of the Bauru Group (Gondwana III Supersequence) in continental conditions (aeolian, fluvial and alluvial environments). From Upper Cretaceous to Early Paleogene times, there was a reduction of the intensity of the tectonic activity.

Faults and fractures analyzed in the present paper were collected in the São Pedro and Botucatu ridges (Figure 3). This region is located at the transition between two large morpho-structural units, the Western Plateau and the Paulista Peripheral Depression (Ross and Moroz [52]), close to the northeastern border of the Paraná Basin, in the State of São Paulo—Southeastern Brazil. The plateau is formed by the Eo-Cretaceous basalt flows of the Serra Geral Formation and the fine aeolian sandstones of the Botucatu Formation. These units are locally topped by sandy to rudaceous deposits cemented by silica and iron oxides (Itaqueri and Marília Formations). The depression developed on the Triassic fine-to-conglomeratic aeolian/fluvial sandstones of the Pirambóia Formation (Caetano-Chang and Wu [53]), which are capped by an Upper Pleistocene colluvial sandy cover (Pinheiro and Queiroz Neto [54,55]). The origin of the large depression and its adjacent plateau is related to the Cenozoic circumdenudation process of the Paraná Basin margins, caused by large rivers entrenched in the old tectonic structures (Ab'Saber [56,57]; Pinheiro [58], and Pinheiro and Queiroz Neto [59]).



Source: DEM: SRTM/NASA, 2000. Geological Survey: CPRM, 2006; PINHEIRO & QUEIROZ NETO, 2016.

**Figure 3.** Geological-structural map of the investigated area with location of the field structural measurement sites (white dots). Base image is the DEM from Shuttle Radar Topography Mission data, 1 arc-second spatial resolution.

## 2.2. Neotectonics of the Northeastern Border of the Paraná Basin

During the last decades, several researches were performed on the structural/tectonic setting of areas that have been traditionally considered tectonically stable. This is specifically true for those regions with economic potentiality related to their (inferred or present) resources, such as hydrocarbons, minerals and groundwater. The Paraná basin is an outstanding example (e.g., Zalán et al. [20]; Milani and Zalán [26]; Milani et al. [22]; Etchebehere et al. [60]). With the aim of unravelling the geological setting of geo-resources embedded in this basin, a large number of investigations have been conducted both at the regional (basin/continental-to-subcontinental) and at the local scale. Studies include the collection of geophysical data as well as field structural measurements (e.g., Milani [37]; Milani and Zalán [26]; Strugale et al. [61]; Costa et al. [62]; Fries et al. [63]). The gathered information revealed the main structural trends of the Precambrian basement and of the Paleozoic-to-Cenozoic covers (Zalán et al. [20]; Hasui et al. [64]), and confirmed the role of inherited weakness zones in the development and following deformation of the basin (Milani [37]; Zalán et al. [10]; Milani and Ramos [43]; Zalán et al. [20]; Almeida [11]; Campanha and Brito Neves [25]; Strugale et al. [61]). Specifically, the inherited crustal weaknesses relate to the Neoproterozoic crustal shear zone and mobile belts that allowed the ancient cratonic assemblage and formation of the Rodina and Gondwana supercontinents (Almeida [23]; Brito Neves and Cordani [24]; Almeida et al. [11]; Campanha and Brito Neves [25]). In the younger (Phanerozoic) tectonic history, these crustal weaknesses were properly oriented with the new tectonic stresses and experienced several stages of reactivations accommodating the intraplate deformation that affected the South America continental plate since the start of the west Gondwana disruption in the Lower Cretaceous (Richetti et al. [33]).

Results of the investigations performed in the last decades evidence the influence of Neotectonics in sculpting the Brazilian landforms (Riccomini [65]; Morales [66]; Etchebehere et al. [60]; Pinheiro et al. [67]; Pinheiro and Cianfarra [68]). A detailed review of the available bibliography (most of which is published in local journals and in reports of private companies/consortia) is far beyond the purposes of the present paper. In the following, we outline the most relevant results that are compared with the outcomes of the present work in the discussion section and support the proposed tectonic model.

The common finding of the performed scientific investigations is that the tectonic framework of the Paraná basin, and specifically of its northeastern margin, is characterized by two main azimuthal trends of structural alignments, namely NE-SW and NW-SE (Soares et al. [18]; Ferreira [69]; Fulfaro et al. [17]; IPT [70]; Zalán et al. [10]; Milani et al., [71]; Zalán et al. [20]; Quintas [72]; Saad [73]; Strugale et al. [61]; Campos et al. [74]; Fries et al. [63]; and Pinheiro et al. [67]). These directions correspond to joints, faults, fault zones, network of faults or shear zones, morphological alignments detected from air photo, lineaments or lineament domains identified on satellite images or else from aeromagnetic and gravimetric images. In most cases, these nearly orthogonal structures affect both the Precambrian basement and the successive Phanerozoic sedimentary cover, and ruled the pathway of volcanic intrusions (dike swarms). Faults and fractures with the same NE-SW and NW-SE directions, cutting through Quaternary deposits were also described at local outcrops in the investigated area (Rostirolla et al. [75]; Morales [66]; Campos et al. [74]; Pinheiro [58]; Pinheiro and Queiroz Neto [54,55]).

A third E-W trending structural direction affecting the study region has been described by authors (e.g., Bjonberg [76]; Curie [77]; Zalán et al. [20], Saadi [78]; Saad [73]; Facincani [79]; Hasui [64]; Pinheiro et al. [67]) and corresponds to morphotectonic directions detected from synthetic scaled images (air photo mosaics or satellite images), faults or fault networks, fault corridors with dimensions ranging from the few meters of single fault at the outcrop scale, to the hundreds of kilometers of the fault corridors and shear zones at the continental or subcontinental scale. Prevailing strike-slip kinematics have been inferred for these E-W structural trends (Morales [66]; Riccomini [65]; Hasui [64]). The existence of regional strike-slip fault strands, nearly E-W oriented and affecting the western Paulista

region (eastern border of the Paraná basin), has been inferred by Saad [73], Riccomini [65] and Etchebehere et al. [60]. Within the deformation zone of this corridor, authors frame the found sinistral movement along NNW-SSE fault set and dextral movement along NW-SE faults. This kinematic suggests a regional dextral shear along the E-W corridor (Riccomini [65,80]). Hasui et al. [64] and Hasui [8] advanced the existence of a regional E-W, strike-slip regime related to the current South America plate drift. Transpressive and transtensive deformation is associated to this tectonic setting along the E-W shear zone. A link has been hypothesized between the E-W trending offshore fracture zones in the South Atlantic (and the nearly parallel on land shear zones located along the same parallel (e.g., Saadi [78]; Hasui [64]; Pinheiro et al. [67]; Vasconcelos et al. [9]; Pinheiro and Cianfarra [68]).

Debate is centered around the age and relative chronology of activity of these populations of structural alignment. Advanced interpretations range between the Phanerozoic reactivation of ancient, crustal weakness shear zones of Proterozoic age (Zalán et al. [10]; Almeida et al. [11]), to a Neotectonic (i.e., Neogene to Quaternary) activity deeply affecting the landscape evolution, and either related to reworking of pre-existing structures or to the formation of new ones (Riccomini [80]; Morales [66]; Santos and Ladeira [81]; Guedes, [82]; Guedes et al., [83]; Pinheiro and Queiroz Neto [54]; Pinheiro et al. [67], Pinheiro and Cianfarra [68]). The found azimuthal trends characterizing the structural grain of the region, also define the borders of basement structural highs, such as Pitanga, Artemis, Pau D'Alho and Jiboia (Sousa [84,85]; Rostirolla et al. [75]; Campos et al. [74]). These dome-shaped structures have been regarded as potential hydrocarbon reservoirs and exploration targets. Again, the formation and evolution of these heights have been alternatively related to reactivation of pre-existing faults (Sousa [85], Morales [66]) or to the activity of fault cutting through the Quaternary deposits (Riccomini [80]; Siqueira [86]). Multiple tectonic events have been recognized also by means of fault slip inversion for paleostress computations (e.g., Fernandes and Amaral [87]). Specifically, the authors identified, among others, two major/regional deformation episodes characterized by a NE-SW main horizontal compression attributed to the Paleogene–Neogene transition, followed by a Quaternary event with NW-SE main horizontal compression. Based on cross-cutting relations of faults and lineaments detected from satellite images and air photos, Hasui et al. [88] and Etchebehere et al. [60] concluded that the NW-SE structures are younger and their movement displaces and rotates the NE-SW structures.

### 3. Materials and Methods

The stress field responsible for the development of brittle deformations (e.g., faults, extensional fractures) results from the (tensorial) addition of various regional and local components. The regional stress component is often referred to as far field stress and is responsible for the development of faults and fractures in the studied region, according to the known various model of failure (e.g., Mohr-Coulomb, Griffith or a combination of the two as proposed by Nicol et al. [89] and Fossen [90]).

Deformations related directly to the regional component can be useful when analyzed by stress inversion techniques to resolve the attitude and shape of the paleostress that produced the failure. The other local stress components are associated to the regional one and can be referred to as secondary or local, due to the wider spatial grade of variability through the region of interest that they have. These local components include the overburden (that is dependent from the local elevation), the topographic slope, the fluid pressure (associated at depth to mineralization to develop veins and dikes) and that produced along faults during their activity by the elastic deformation of rocks induced by friction or elastic accumulation within their elasto-frictional behavior.

This last local component has well-defined geometric relations to the generating regional fault and concentrates along and nearby, where it often results the strongest. This zone (the fault deformation zone, e.g., Caine et al. [91]) is characterized by the development of sets of brittle fractures (commonly referred to as Riedel fractures, e.g., Fossen [90]), whose

geometry is therefore related to the fault activity rather than to the regional stress. In this case, their inversion would result in the geometry of this component, and its comparison with the geometry of the generating fault allows for inferring its kinematics.

In the present work, we will refer to the stress responsible for the main, regional fault as dynamic stress, and to the (local) stress produced by the fault movements as the kinematic stress. These terms simplify the description since any fault may act as a main element and let the development of secondary fracturing by its movement (in this case, these deformations would have been produced by the associated kinematic stress). It is worth noting that this relation (dynamic versus kinematic stress) can be applied to any scale of analysis. Once identified and separated, the analyses of the two fault groups allows for the guessing of the paleostress geometry that acted during the tectonic evolution of a region, as well as the kinematics of the larger, main faults that are present. The main difference between the two sets is the obvious sub-ordered dimension of the kinematic-related fractures with respect to the main, generating one.

Obviously, the attribution to dynamic versus kinematic conditions of fractures at a given scale is not an easy task. The sub-ordered dimension and their increasing in size and frequency by approaching the main responsible fault are a good indicator, as well as their geometry in approaching the regional fault. Kinematically induced faults and fractures will never cut-cross their generating fault, and, by approaching it, they show a change in their attitude to face the main fault displacement. As an example, synthetic cleavage faults (e.g., R-type Riedel Fracture) will tend to rotate and lie parallel to the main fault to constitute the characteristic “recorder beak” or “bico de flauta” geometry (Figure 4). On the other hand, antithetic cleavage faults will rotate to a higher angle when joining the main fault.

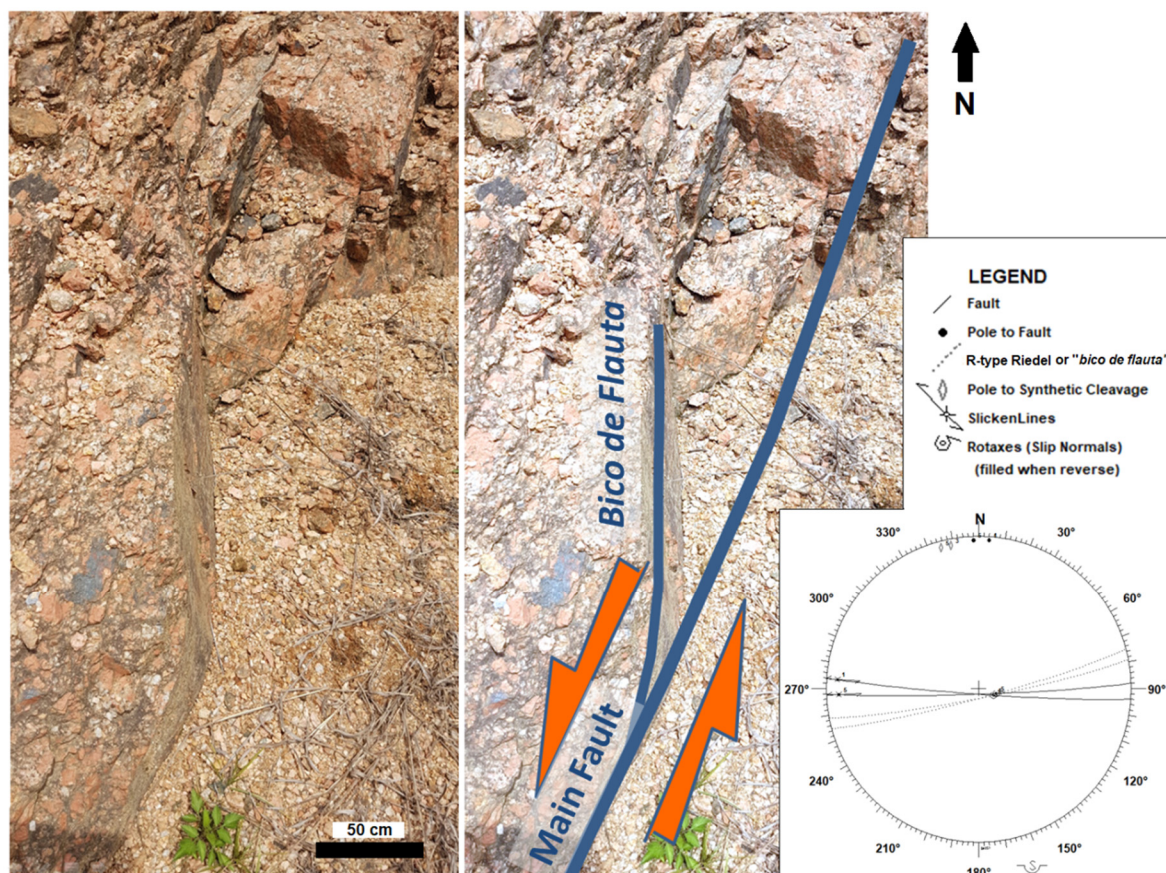


**Figure 4.** Example of strike-slip fault in Precambrian granites with associated R-type Riedel fractures or “bico de flauta” showing a left-lateral kinematic. Note the rotation of the “bico de flauta” azimuth when approaching the main fault and the nearly parallel attitude where they joint.

These, and other geological considerations, i.e., the compatibility with the kinematics of main fault as derived from other indicators and with a proposed geotectonic model, allow in most cases to solve this puzzle. It is worth mentioning that any fault and fracture produced by the kinematic stress along a major element joins it along a line that is always parallel at the null axis of the latter (rotax, Salvini and Vittori [92], or slip normal) and its normal vector on its plane is always an indication of the kinematic vector.

In order to highlight the tectonic setting of the investigated region, structural elements (e.g., faults and extensional fractures) have been collected and analyzed on stereonets to obtain their attitude distribution. The collected fault and fracture attitudes were also statistically analyzed by a polymodal Gaussian fit to identify the principal azimuthal family sets (Cianfarra and Salvini [93]). Paleostresses orientations by fault and fracture inversions were performed to identify the regional deformation history. The statistical analyses and fault and fracture inversion have been performed using the Daisy3 freeware (v.522\_e, Salvini et al. [94]; <http://host.uniroma3.it/progetti/fralab/> accessed 29 November 2021).

Fault kinematics have been determined from the kinematic indicators on the fault plane (e.g., slickenlines, striations), but also from the intersection and relative attitude of the fault-related fractures (i.e., Riedel planes). This process allows to compute the fault kinematic vectors and rotaxes (Salvini and Vittori [92], i.e., slip normal or rotational axis, Wise and Vincent [95]), a vector that approximate the  $\sigma_2$  orientation in faults related to dynamic stress conditions, that is in faults generated, in the study area, by the regional stress with the potential generation of possible conjugate set. According to their generation, faults related to dynamic stress are characterized by a higher rotax clustering than slicks and pole-to-planes. On the other hand, the attitude distribution of faults related to kinematic stress (e.g., discontinuities between blocks produced by their relative movement) is characterized by a relatively higher clustering of the kinematic vectors (fault slicks) than fault rotaxes and poles-to-plane, since the fault displacement tends to ease the relative movement vector between adjacent blocks along a preferential orientation. In this way, the comparison between the scattering of kinematic vectors and rotaxes allows to identify faults related to dynamic vs. kinematic prevailing type of paleostress. The former faults can be statistically analyzed and inverted for paleostress determinations, while the inversion of the second group can be effectively used to identify the kinematics of regional faults in the studied area.

Extensional stress condition is often responsible for the development of open extensional fractures/joints (as well as dikes and veins at depth, when the contribution of fluid pressure eases the rock failure). It is very common to observe that this activity produces two sets of nearly orthogonal fracture systems and leaves ambiguity in recognizing the direction of the regional extension direction (Caputo [96]). In this study, we present a methodology that provides the stress field inversion of near-orthogonal extensional fracture sets (hereafter referred as joints) by the identification of systematic versus non-systematic fracture system (Price and Cosgrove [97]) in rocks with viscoelastic behavior (e.g., due to the velocity of brittle deformation development, they react as a brittle material during faster deformation and as a ductile one for low-velocity deformation, Turcotte and Schubert [98]). It is worthwhile to notice that the two sets are both the deformation associated to a single tectonic event with a given regional stress. Specifically, the population of joints clustered along the preferential direction with the smaller azimuthal scattering (quantified with its standard deviation—sd) is hereafter referred to as the systematic joint set and it is considered that it develops mostly before the non-systematic set. This produces a general hierarchical abutting of the younger non-systematic fractures against the pre-existing systematic ones (Figure 5). Since the development of non-systematic fractures generally starts when the formation of the systematic fractures is still ongoing, a small quantity of opposite abutting can also be observed (refer to Figure 6 for the evolution though time of the two systems). On the other hand, the nearly orthogonal joint population characterized by the highest sd of the azimuthal directions and with the smallest mean cumulative length is the non-systematic set (e.g., Pinheiro et al. [67]). This last usually extends across the intervals between the preexisting joints of the systematic set and terminate at nearly right angles

to them (Gross [99]). The wider scattering results from the deviation of the stress field disturbed by the systematic fractures.

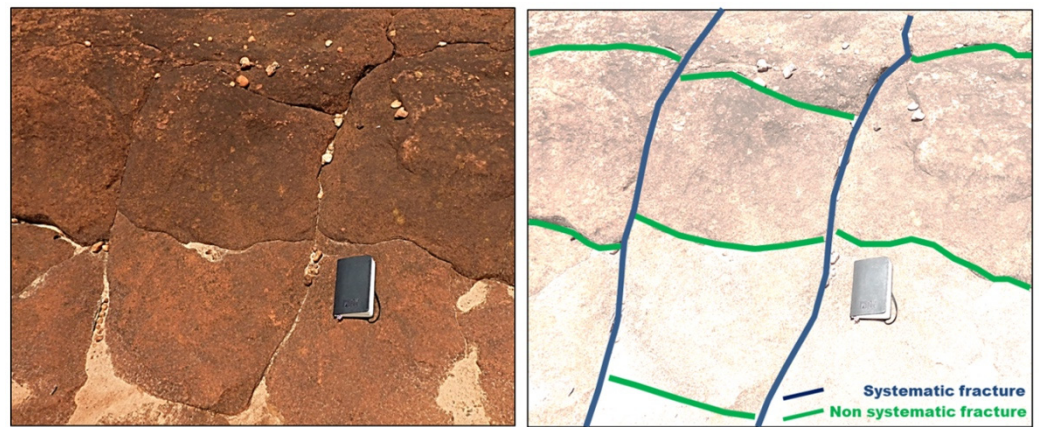


Figure 5. Example of nearly orthogonal systematic and non-systematic fractures in Upper Pleistocene continental sand deposits (Location: 22°34'23" S, 48°01'49" W).

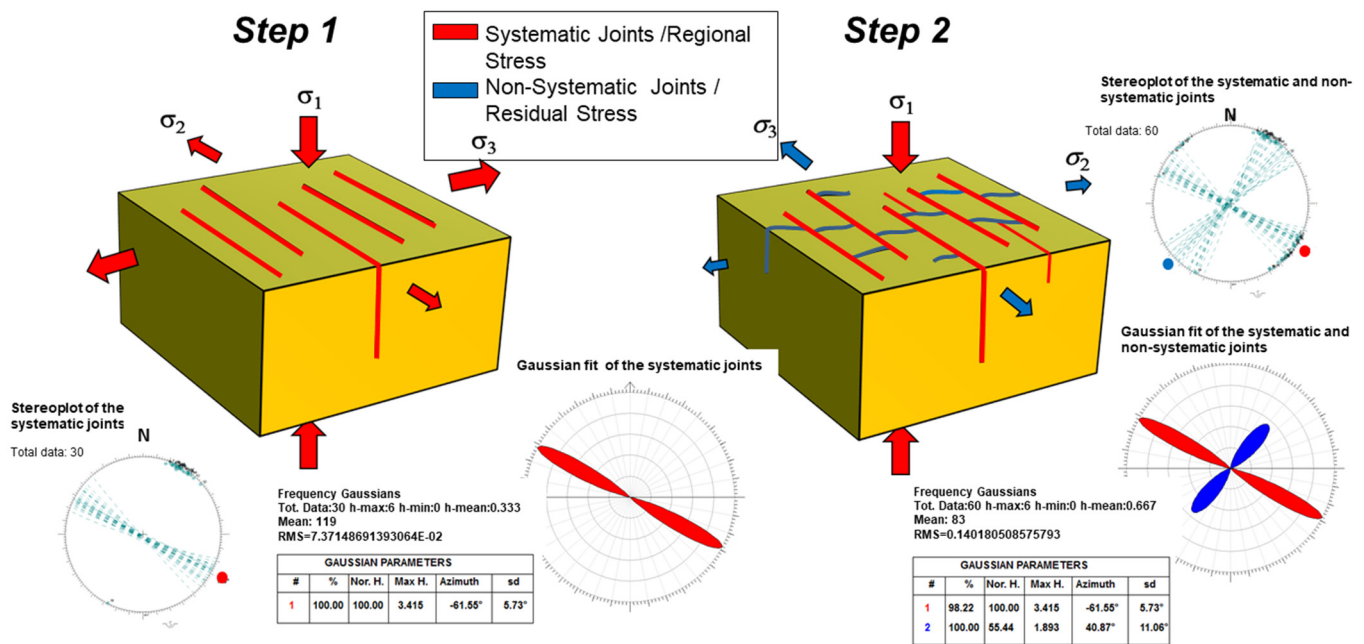


Figure 6. Development of systematic and non-systematic near-orthogonal joint systems. During Step 1 we assist to the initial development of the systematic joint set (i.e., normal to the  $\sigma_3$  component). During the successive Step 2, non-systematic joints develop and interact with both pre-existing and newly developed systematic joint to form the nearly orthogonal joint sets (see text for explanation). Data are projected on Schmidt Net (lower hemisphere) by Daisy 3 software. Wind-roses show the Gaussian fit of their azimuthal frequency.

The computation of the paleostress responsible for the development of near-orthogonal joint systems derives from the model of their formation (Figure 5).

The outcropping sedimentary rocks, where the measured fractures develop, can be considered a classical viscoelastic material (Turcotte & Schubert [98]). This means that, depending on the velocity of deformation, they react as a brittle material during faster deformation, and as a ductile one for low-velocity deformation. The critical boundary velocity between these two behaviors is very sharp, since the development of fractures and the subsequent total elimination of the stress component normal to them prevents

from further ductile deformation along this trajectory. This is also eased by the fast (rather instantaneous) development and propagation of fractures. This behavior allows to treat the rheology of the rocks affected by fracturing as an elastic-frictional material and to invert/process them and detect the responsible paleostress likewise. Poorly consolidated fine-grained materials are characterized by a relatively low cohesion and strength. As a result, these rocks are characterized, for the same applied stress, by a strain rate higher than those of consolidated rocks. Two more features characterize cohesionless granular material and ease the development of faults (Balsamo et al. [100]). Grains are allowed to roll and this greatly reduces the friction on a fault plane (as it happens in cataclases). Secondly, the inhomogeneity associated to granularity, and specifically for larger grain size, results in the scattering of the displacement within a deformation band.

We assume that extensional tectonics produces stress values progressively close to the critical fracture failure conditions that are with a negative  $\sigma_3$  with a module just lower than the rock tensile strength. In this situation, a local or random coherent stress variation (including the propagation of seismic waves) will provide the extra stress necessary (a negative component parallel to the  $\sigma_3$  in our case) and produce an extensional fracture normal to the maximum extensional stress component ( $\sigma_3$ ). As the fracture develops, the stress component normal to it will reduce to almost zero, thus preventing the development of a nearby successive fracture and partly rotating the stress tensor in the surrounding area. As a quantitative example, consider near-failure conditions for an extensional stress near the surface with a vertical  $\sigma_1$  of 10.0 MPa (corresponding to the overburden of about 500 m), and an extension (minimal horizontal stress,  $Sh_{min}/\sigma_3$ ) of -5.9 MPa oriented N-S (conventionally, positive values of stress are assumed to be compressive, while negative are tensional). In this example, the maximum horizontal stress  $Sh_{max}/\sigma_2$  will be E-W oriented (i.e., normal to the other two principal stress conditions) and with a negligible value around 0.0 MPa. As an accidental stress propagates in the rock and provides an extra  $-0.1$  MPa in the N-S direction, the resulting stress will override the tensile strength of the rock and an E-W joint set will develop. This process will produce in the whole rock a joint system oriented normal to the regional extension. This corresponds to the systematic joint system, which is characterized by a mean E-W orientation (normal to the mean acting regional  $\sigma_3$ ) and a given azimuthal standard deviation  $sd$ . At this stage, the stress component normal to the joint will reduce to almost 0, and the new stress tensor will still preserve a vertical  $\sigma_1$  of 10.0 MPa, and the two horizontal components (in this example!) will decrease to 0.0 MPa (no extensional stress can be transmit normal to it).

The continuation of the regional stress activity in the region on the newly fractured rock will always have a near 0 value normal to the fracture, but some extensional component will easily develop at a high angle to the joint, since its potentiality in reducing the extensional component is maximum for the direction normal to the joint, and progressively decreases as this angle become smaller (down to 0 for the stress direction parallel to its plane).

In this condition, it is expected that a small extensional component related to the regional tectonic activity may easily develop in the direction nearly parallel to the existing joint system. The interaction between the null stress component produced by the systematic joint system normal to it and the acting stress results in the development of a new value and orientation of stress tensor. It is characterized by the same vertical  $\sigma_1$  (10.0 MPa), a 0.0 MPa null stress along the normal of the systematic joints and a decrease of the extensional stress around the horizontal direction parallel to the systematic joints. This direction becomes the new  $\sigma_3$  and progressively reaches, with the contribution of local stress components, the tensile strength conditions and a new set of joints, nearly orthogonal to the former one, develops.

The attitude of this new joint set will generally not be precisely normal to the previous one, since it may be influenced by: (i) the presence of the systematic joints that prevent from the development of a smaller negative stress value normal to it; (ii) the channelization of the regional stress along the path (azimuth) of the systematic joints due to the new mechanical property generated; and (iii) the development of some shear component along

the systematic joints. These perturbations likely produce a larger variability in the local stress orientations and therefore on the orientations of the fractures of the new set. This results in a wider sd of their attitude distribution than the former system, and for this reason it is referred to as the non-systematic joint system.

The difference in their standard deviations (sd) may be used to identify in the fracture set, which of the orthogonal joint system, represents the systematic one, when it is not possible to recognize in their intersections a chronological/hierarchical order (i.e., the younger, non-systematic extensional fracture stops when intersects a pre-existing one, typically a systematic fracture, due to the high angle between the two systems). Very often in the field, the two systems do not form a perfectly averaged  $90^\circ$  angle and observed values range between  $70^\circ$ – $90^\circ$ . As abovementioned, this may derive from the characteristics in the development of non-systematic joints.

It is important to notice that in any conditions and if the two systems develop under the persistence of the same regional stress conditions, the line of intersection between the mean planes of the two systems correspond to the attitude of the main principal component  $\sigma_1$  of the responsible stress. Again, the successive development of the non-systematic versus the systematic joint systems has to be intended at the local scale (i.e., nearby the systematic joint). As we can easily observe in the field by looking at fracture intersections, a non-systematic fracture propagated from an older systematic fracture, can interrupt a successive systematic one. This easily provides several orders in the chronological order and unravelling the time sequence of the two systems is not easily accomplishable.

A brief introduction to the adopted inversion methodologies of faults and extensional fractures is reported in the following.

### 3.1. Monte Carlo Direct Inversion

The paleostress inversion of all faults was aimed to identify the minimum number of possible paleostress events that produced the measured fault populations following the approach presented in Pinheiro and Cianfarra [68]. This has been accomplished by the application of a Monte Carlo convergent methodology (e.g., Tarantola [101]) to the fault inversion that provides the best attitude of the principal paleostress components ( $\sigma_1$ ,  $\sigma_2$ ,  $\sigma_3$ ) with an estimate of the associated error. The error is quantified by the MAD (mean angular deviation) factor, that is the average angular deviation between the measured pitch of the kinematic vector on the plane and the predicted one by applying to the fault the computed paleostress. This methodology looks for the best dynamic paleostress conditions (as above defined) responsible for the (re)activation of all faults.

The Monte Carlo direct inversion that considers a single paleostress event to generate all faults is based on the successive comparison with a huge number of randomly generated stress tensors and rheological properties. At each step, the reliability of the proposed values is evaluated by computing the MAD of the given fault population.

At each comparison, the obtained MAD is compared with the least value found, and if lower, the new paleostress parameters and its MAD are memorized as the temporary best fit. This comparison is repeated for cycles of a pre-determined number of attempts (20,000 for our analysis), until no better conditions are found within the last cycle. At each cycle, the range interval of randomly generated factors is reduced around the best found values. This guarantees the generation of new sets of random values, thus converging and improving the Monte Carlo best fit. The final result represents the best stress that explains the analyzed fault population. The reliability of the fit is evaluated by the final MAD value. Generally, a value lower than  $40^\circ$  may be considered reliable, providing that re-activation of pre-existing fault planes can occur within that difference (Nur et al. [102]).

The multiple-stress Monte Carlo direct inversion works similarly. In this case, at each attempt, a set of  $n$  paleostress fields are generated and faults are compared to each of them. The faults are then associated to the paleostress that provides the least angular difference between the measured kinematic vector and the expected one. At the end of the attempt, a MAD is computed as well as the association of the faults to one of the  $n$  paleostresses.

This attempt is repeated for a predetermined number of times (10,000 multiplied by the number  $n$  of paleostresses,  $n = 2$  in our final case, that provides 20,000 attempts at each cycle). The Monte Carlo inversion ends when no reduction in the MAD occurs in the last cycle of attempts. The obtained paleostress values are recorded and faults are classified on the basis of the associated paleostress event when their angular deviation is lower than a given angle (a classification default value of  $30^\circ$  was chosen in our analysis).

Typically, the multiple-stress Monte Carlo approach is conducted by performing a series of inversions with the progressively increasing number of “concurrent”  $n$  paleostresses until an acceptable MAD is reached (typically  $<40^\circ$ ). It has to take into serious consideration that each increment in the number of paleostress reduces the degrees of freedom (DOF) of the inversion process, thus lowering the robustness of the results.

### 3.2. Inversion of Near-Orthogonal Fracture Systems

According to the development model presented above, the procedure for stress inversion of near-orthogonal joint systems is straightforward: to identify which of the systems represent the systematic one. The  $\sigma_3$  will lie along the normal of the average attitude of that system. Although it looks rather simple, the inversion has to solve both the stress orientation and the grouping of the fractures into the two families (i.e., systematic versus nonsystematic). This prevents the use of classical/deterministic inversion methods (as those based on the least square method).

The approach used in the present paper is again the classical presented Monte Carlo, i.e., the software routinely generates random stress tensors. Each of these stresses is then applied to all the joints and a deviation angle is computed between the stress tensor and the normal to the joints. This comparison is conducted twice, with the  $\sigma_3$  orientation (if the joint is a systematic one), and with the  $\sigma_2$  (in case the joint is a non-systematic). The smaller angle will provide the identification of the fracture and will be kept. The average values of all fractures will provide the mean angular deviation, MAD.

This iteration is repeated at cycles of 10,000 times and the least value of MAD and the relative stress tensor is recorded. As no reduction of MAD occurs after a cycle, the resulting parameters are considered reliable and provide the final result. In the application of this study, the no-improvement number of attempts at each cycle was fixed at 10,000. That is, the program starts with the first 10,000 random parameter set (first cycle). Then, it again runs testing 10,000 further parameter sets (successive cycle). If a reduction in the MAD occurred, a new cycle is conducted. This keeps on until no better (smaller) MAD is computed during the last cycle. Larger numbers of attempts were tested but provided nearly identical results. The ambiguity in the identification of the joints may be overridden if field observations allow for identifying the pertaining of a fracture to one of the two sets. In this case, the inversion process can be set to force the observed pertinence for the given joint.

## 4. Results

### 4.1. Fault and Fracture Data Presentation

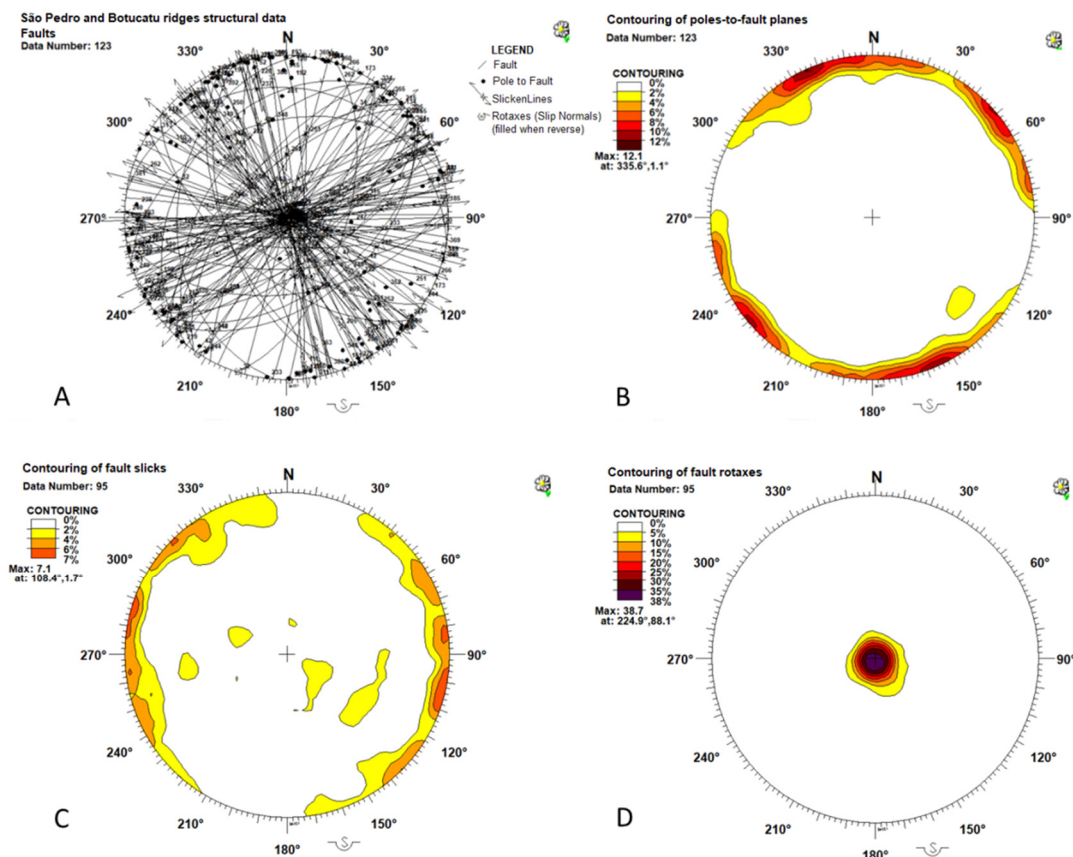
A total of 511 structural field measurements were collected in the investigated area from 45 selected sites (Figure 3). Analyzed structural data include faults (No. 123 fault planes with their kinematics), joints (No. 227 fracture planes), fault-synthetic cleavages (No. 83 Riedel R-planes), shear fractures (No. 69 cleavage planes), morphological alignments (No. 2 data) and beddings (No. 7 bedding planes). Data from all the field measuring stations were cumulated and statistically analyzed, separating faults, joints, fault-synthetic cleavages (Riedel R-planes) and shear fractures. The intersection and relative attitude between faults and their associated synthetic/antithetic fractures (Riedel R/R'-planes) allowed the determination of the fault kinematics and to compute the fault kinematic vectors (Figures 4 and 7).



**Figure 7.** Example of faults measured in the field with associated brittle deformation (R-type Riedel synthetic fracture or “bico de flauta” and/or R'-type antithetic fracture). A. Right-lateral strike-slip fault in sandstones of the Piramboia Fm at the Piracicaba river (Location:  $22^{\circ}37'06''$  S,  $48^{\circ}05'25''$  W). B. Left-lateral strike-slip fault in diabase Serra Geral Fm outcropping at the escarpment of the São Pedro Ridge (Location:  $22^{\circ}30'11''$  S,  $48^{\circ}11'53''$  W). Data are projected on Schmidt Net (lower hemisphere) by Daisy3 software.

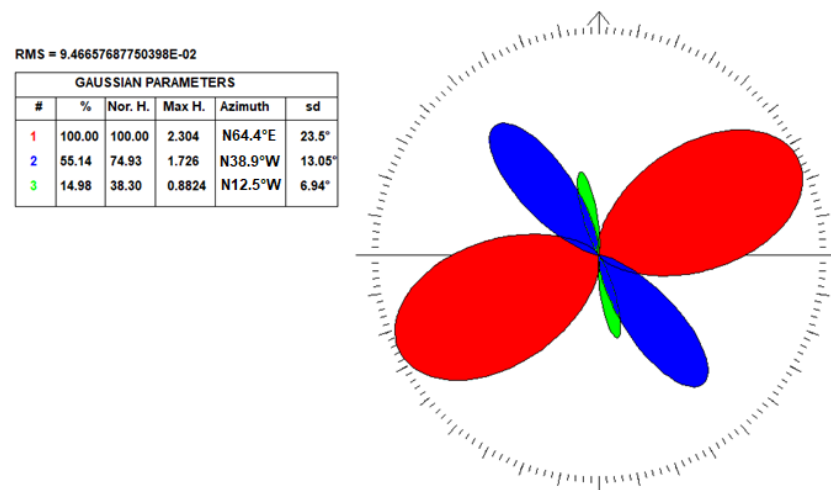
The chosen strategy to statistically analyze the cumulated structural dataset neglecting the specific position of each field site allowed the highlighting of the regional/geodynamic structural trends of the investigated region. The local spatial variability of the measured fault and joint trends were considered the result of the addition of the regional tectonic stresses and of the local scale factors that are negligible in the preparation of the regional tectonic evolutionary model of the studied area. We expect that the regional tectonic stresses active during the geodynamic evolution of the study area produced a (brittle) deformation signature that spatially presents common azimuthal trends with only minor rotations/deviations. On the other hand, the local spatial variations will affect the results of the cumulated statistical analyses in terms of data scattering. Alternatively, if we consider only the last plate scale tectonic event, the angular dispersion may stem from the rotation of the previous structures accommodating the modern stress field. In this way, finding systematic clusters of azimuthal families in the analyzed fault and fracture populations confirms the validity of the chosen approach. This strategy of regionally, cumulated fault and joint inversions was followed to infer the regional tectonic stresses ruling the recent-to-present structural evolution of the region in the framework of the regional geodynamics.

Figure 8A shows the stereoplot of the 123 faults with their kinematic vectors. Contouring of pole-to-fault planes highlights that all the measured faults are nearly sub-vertical and cluster in two main family sets trending NW-SE and NE-SW (Figure 8B). Notably, these two fault sets are nearly parallel to the main trends of the regional/basin scale faults (derived from literature e.g., Zalan et al. [20]) as those represented in Figure 2. This suggests that our fault data follow the regional structural grain and are representative of the main structural and tectonic trends.



**Figure 8.** Total fault analysis. (A). Stereoplot of fault planes and fault pole-to-plane with their kinematic vectors. (B). Contouring of pole-to-fault planes. (C). Contouring of the fault slicks. (D). contouring of fault rotaxes. Data are projected on Schmidt Net (lower hemisphere) by Daisy3 software.

Contouring of the fault slicks shows their sub-horizontal plunge with an average orientation around WNW-ESE (Figure 8C). Contouring of the fault rotaxes show the cluster of vertical  $\sigma_2$  (Figure 8D). This last result strongly suggests that a main strike-slip tectonic setting affected the investigated region. The polymodal Gaussian fit of the 123 measured faults shows their clustering in two main azimuthal sets: the main one is N64°E oriented, the second is N39°W oriented. A sub-ordered third set is also present and is N13°W oriented (Figure 9).



**Figure 9.** Results of the Polymodal Gaussian Fit of the total measured faults.

Part of the measured fault population propagated within Quaternary deposits. Figure 10 shows an example of conjugate reverse faults that cut through the Permian siltites of the Corumbataí Formation and the Quaternary fluvial conglomerate. These faults are NE-SW trending and displace the original contact/boundary between the siltites and the continental conglomerates. At this field measurement site, an E-W trending right-lateral strike-slip fault is also present.

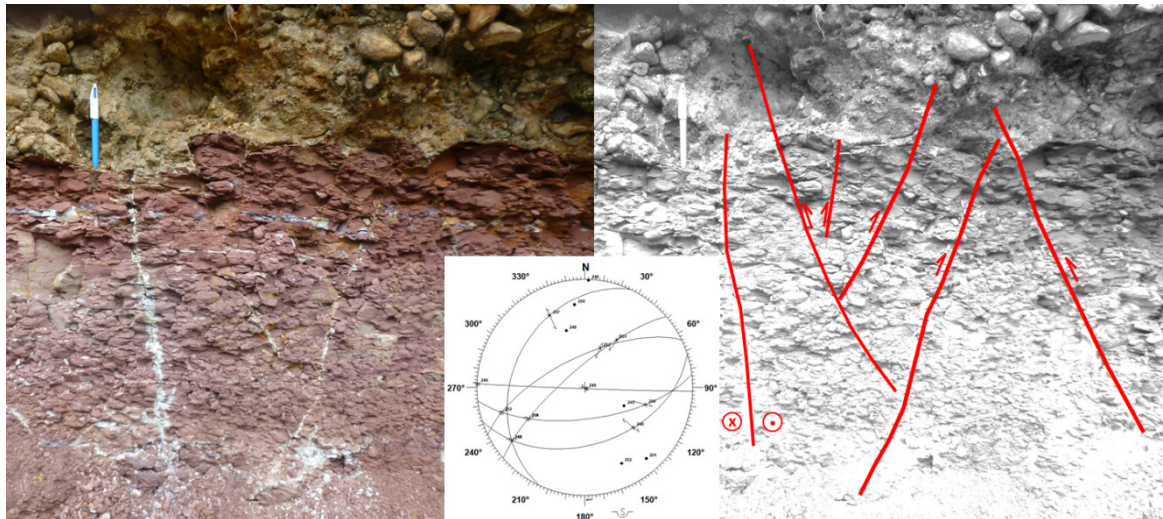


**Figure 10.** Quaternary fluvial conglomerate upon Permian siltites (Corumbataí Formation) displaced by conjugate reverse faults trending NE-SW. Data are projected on Schmidt Net (lower hemisphere) by Daisy3 software. (Location: 22°25′52″ S, 47°41′48″ W).

A total of 227 joints were measured and are characterized by sub-vertical dip (Figure 11). The stereoplot of the joints (Figure 11A) and the contouring of their pole-to-planes (Figure 11B) shows that they cluster in two nearly orthogonal azimuthal families, NE-SW and NW-SE oriented. This result is confirmed by the polymodal Gaussian fit showing their clustering in two azimuthal families trending N54°W and N42°E (Figure 11C). The latter family is characterized by the higher scattering (standard deviation  $sd = 25^\circ$ ) with respect to the first family ( $sd = 16^\circ$ ). This azimuthal arrangement and data scattering is compatible with the systematic and non-systematic fracture organization, being the NW-SE more clustered set associated to the systematic family. The analysis of the joints cutting the Quaternary deposits (e.g., Figure 5) provided similar results (Figure 11D) with one, more clustered, azimuthal family set trending N56°W ( $sd = 15^\circ$ ) and the other more scattered, azimuthal family trending N35°E ( $sd = 19^\circ$ ). Although the difference in angular scattering is relatively small ( $4^\circ$ ), the NW-SE joint set corresponds to the systematic set, and the NE-SW to the non-systematic one.

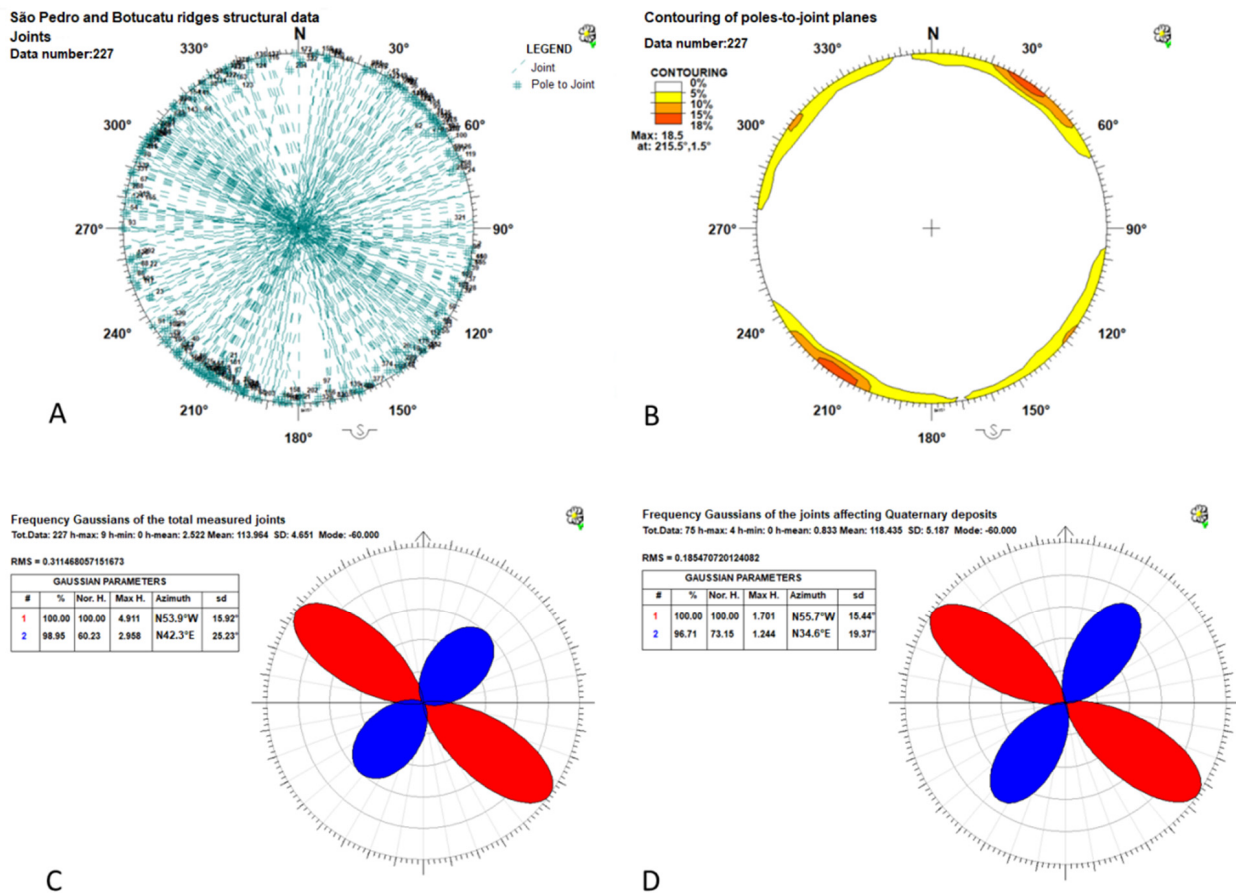


**Figure 11.** Joint analysis (A). Stereoplot of the total measured joints. (B). Contouring of the total pole-to-joint planes. (C). Polymodal Gaussian fit of the total joint planes. (D). Polymodal Gaussian fit of the joints affecting the Quaternary deposits. (A,B): Data are projected on Schmidt Net (lower hemisphere) by Daisy3 software.

The stereoplot and the pole-to-plane contouring of the 69 shear fractures show that they cluster in two sub-vertical azimuthal families N-S and E-W oriented (Figure 12A,B). Again, a nearly orthogonal relation exists between the found azimuthal set and is confirmed by the polynomial Gaussian fit analysis showing two main trends oriented N5°E and N89°E, respectively (Figure 12C). The abutting relationship between these two sets of shear fractures suggests that they are coeval. This strengthens our model with almost coeval high-angle joint sets.

The 83 fractures (Riedel R-planes) are characterized by a nearly vertical dip (Figure 13A,B), that compared with the similar vertical attitude of the measured faults, provide vertical rotaxes/ $\sigma_2$  and confirms the prevailing strike-slip motion. As expected, the synthetic fractures (Riedel R-planes) cluster in two azimuthal families, nearly orthogonal, NW-SE and NE-SW oriented (Figure 13C). The results of the polymodal Gaussian fit of these structural features showed two main peaks N53°E and N49°W oriented.

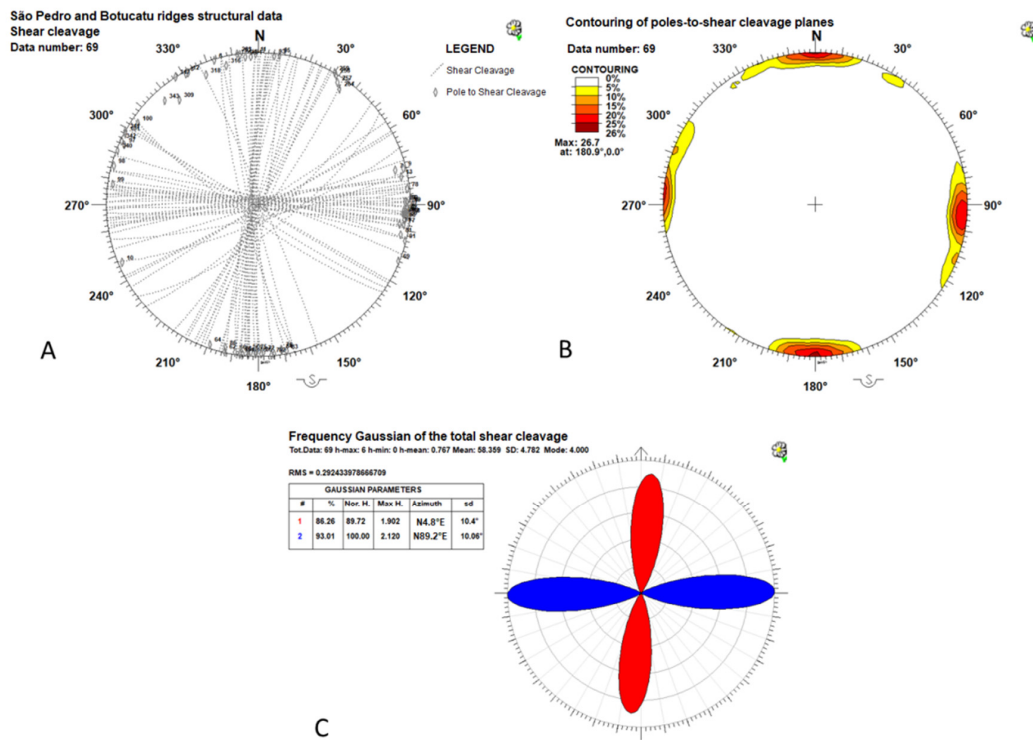


**Figure 12.** Total shear cleavage analysis (A). Stereoplot of the measured shear cleavages. (B). Contouring of the shear cleavage pole-to-planes. (C). Polymodal Gaussian fit. (A,B): data are projected on Schmidt Net (lower hemisphere) by Daisy3 software.

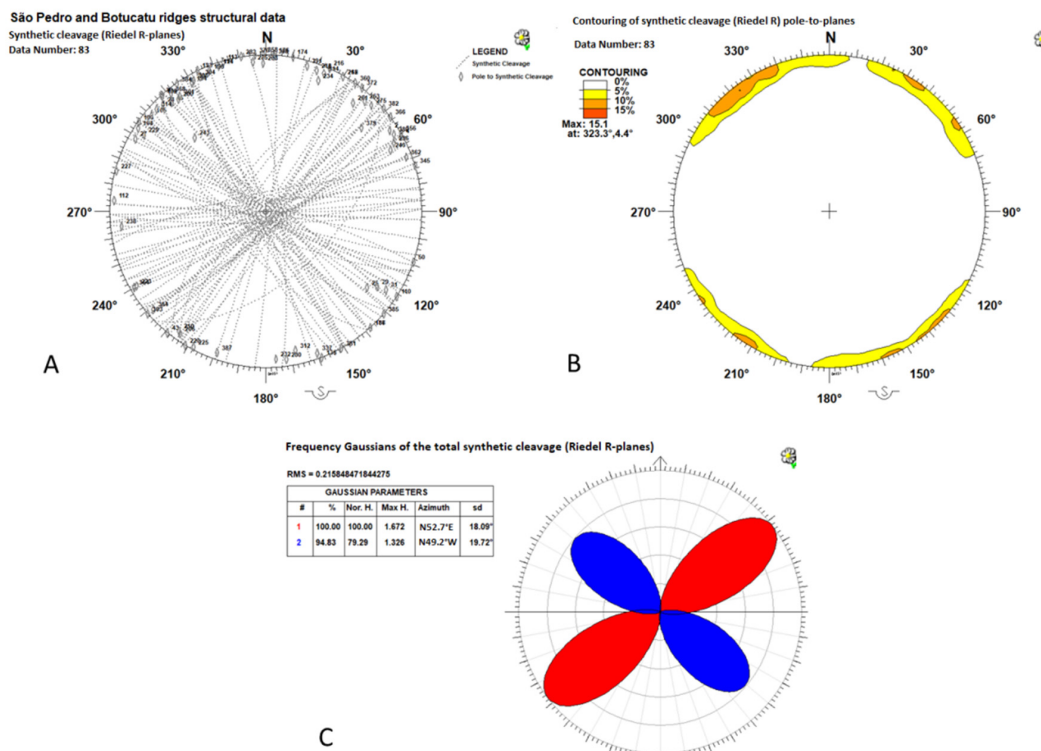


**Figure 13.** Total synthetic cleavage (Riedel R-planes) analysis and polymodal Gaussian fit. (A). Stereoplot of the synthetic cleavage planes and pole-to-planes. (B). Synthetic cleavage contouring of the pole-to-planes. (C). Polymodal Gaussian fit. (A,B): data are projected on Schmidt Net (lower hemisphere) by Daisy 3 software.

#### 4.2. Faults and Extensional Fractures Inversion

Fault inversion was performed by the multiple Monte Carlo direct inversion approach. Firstly, an inversion aiming at identifying a single paleostress was conducted and the result was not considered reliable since the computed MAD ( $83^\circ$ ) was considerably higher than the acceptable  $40^\circ$ . Successively, a fault inversion was accomplished to obtain two paleostress events for the measured fault population. The results are shown in Figure 14. One event (MAD =  $35^\circ$ ) is characterized by an extensional tectonic regime (sub-vertical  $\sigma_1$ , plunging  $80^\circ$ ) with the minimum horizontal stress ( $\sigma_3$ ) N $62^\circ$ W oriented (plunging  $8^\circ$ ) and the maximum horizontal stress ( $\sigma_2$ ) N $29^\circ$ E oriented (plunging  $5^\circ$ ). The other paleostress (MAD =  $37^\circ$ ) indicates a strike-slip tectonic setting (vertical  $\sigma_2$ , plunging  $88^\circ$ ) with the minimum horizontal stress ( $\sigma_3$ ) N $32^\circ$ E oriented (plunging  $1^\circ$ ) and the maximum horizontal stress ( $\sigma_1$ ) N $58^\circ$ W oriented (plunging  $1^\circ$ ).

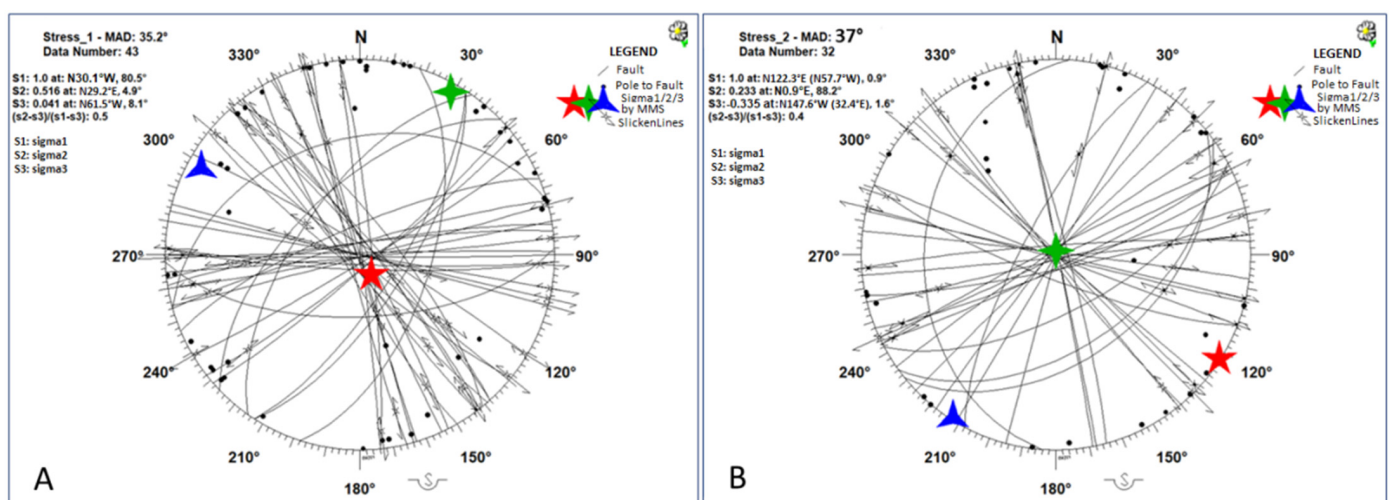


**Figure 14.** Results of multiple Monte Carlo fault inversion showing the two paleostresses characterized by the switch of the minimum and maximum horizontal stress component. (A). The first solution is characterized by NW-SE minimum horizontal stress component and NE-SW trending maximum horizontal stress component, (B). The second solution is characterized by NW-SE maximum horizontal stress component and NE-SW minimum horizontal stress component. Data are projected on Schmidt Net (lower hemisphere) by Daisy3 software.

Paleostress computation by extensional fractures inversion provided a result similar to the latter paleostress event computed by fault inversion (Figure 15). Specifically, inversion of the classified systematic and non-systematic joint set (according to Figure 11C) provided a reliable solution (MAD =  $10^\circ$ ) characterized by the minimum horizontal stress ( $\sigma_3$ ) N $37^\circ$ E oriented (plunging  $0.3^\circ$ ) and the maximum horizontal stress ( $\sigma_2$ ) N $53^\circ$ W oriented (plunging  $0.3^\circ$ ) with a vertical  $\sigma_1$ .

In order to provide a temporal constraint to the poly-phased tectonic history arisen by the fault inversion, extensional fractures affecting Quaternary deposits (e.g., Figure 5) were separately analyzed (Figure 16). A total of 48 extensional fractures (out of 138 fractures) were inverted and the reliable solution obtained is characterized by a MAD of  $10^\circ$  with the minimum horizontal stress ( $\sigma_3$ )  $143.7^\circ$ W/N $36^\circ$ E oriented (null plunging) and the maximum horizontal stress ( $\sigma_2$ ) N $126^\circ$ E/N $54^\circ$ W oriented, and a vertical (plunging  $89^\circ$ )  $\sigma_1$ . This solution is almost equivalent to the previous one related to the whole fracture population with only  $1^\circ$  rotation of the horizontal principal tensor components.

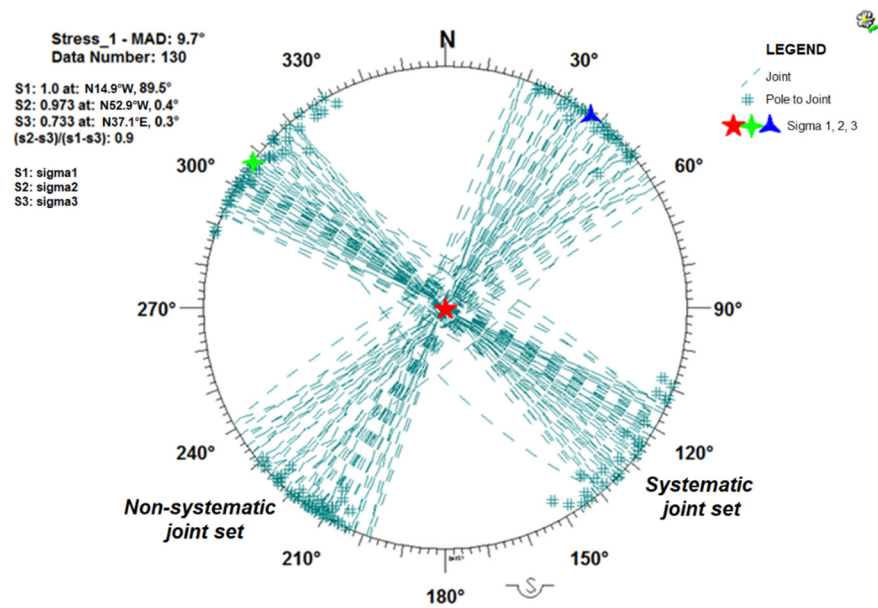


Figure 15. Results of Monte Carlo direct inversion of the classified systematic and non-systematic joints. Data are projected on Schmidt Net (lower hemisphere) by Daisy 3 software.

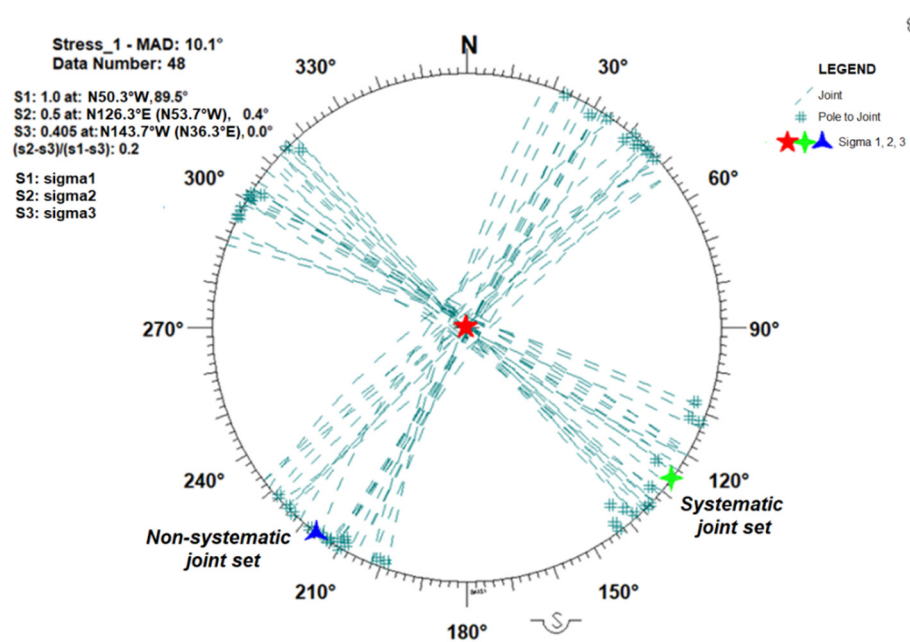


Figure 16. Results of Monte Carlo direct inversion of the classified systematic and non-systematic joints affecting the Quaternary deposits. Data are projected on Schmidt Net (lower hemisphere) by Daisy 3 software.

### 5. Discussion

The adopted original approach of direct inversions by multiple Monte Carlo method allowed the identification of a poly-phased tectonic history that affected the NE border of the Paraná basin. Two paleostress events were computed by fault inversion (Figure 14), one characterized by NW-SE minimum horizontal stress and NE-SW maximum horizontal stress in a general extensional regime (sub-vertical  $\sigma_1$ ), the other event is characterized by NW-SE main horizontal stress and NE-SW minimum horizontal stress in a strike-slip tectonic regime (vertical  $\sigma_2$ ). This last tensor is compatible with the solution resulting from the extensional fracture inversion (Figure 15) characterized by NE-SW minimum

horizontal stress and NW-SE maximum horizontal stress. Inversion of fractures cutting the Quaternary deposits (Figures 5 and 16) confirmed this last solution and allowed the identification and characterization of the youngest/last tectonic event affecting the study region. Moreover, this also supports our method for defining systematic vs. non-systematic joint sets.

Other considerations strengthen the obtained results and confirm the Neotectonic activity in the area. The extensional fracture systems found easily represent the youngest brittle deformation episode in the study area. This derives from a series of considerations. These fractures are open, i.e., without mineral filling that testifies their development without a significant mineral bearing fluid circulation (fluid pressure). This means that the responsible stress (the  $\sigma_3$ ) had a negative value. This combines with the uniaxial strain conditions derived from the overburden conditions that produces a positive increment in final stress tensor with a typical vertical increment due to the overburden  $S_v$  ( $S_v = \rho g h$ , where  $\rho$  is the rock density,  $g$  is the acceleration of gravity,  $h$  is the burial depth) and a corresponding horizontal stress component ( $S_h$ ) of the order of one third of the vertical component  $S_v$  ( $S_h = S_v * \nu / (1 - \nu)$ , with  $\nu = 0.25$  is the Poisson's ratio). This prevents the development of tensile stress even at small depth (some tents of meters). In this way, the observed extensional fractures developed in a near surface environment.

Due to the high erosional rates in the study area (Pinheiro and Queiroz Neto [47]), surface rocks are preserved for a relatively short time before being eroded away together with their embedded deformation. Therefore, the observed fracture systems have a relatively younger age. On the other hand, faulting is a process that best develops under (positive) stress conditions when the difference between the maximum and minimum stress components produces a shear that overrides the strength of the rock (Mohr-Coulomb criterion). As a result, they can initially develop at a depth where the overburden provides the required stress increment. In this way, the observed faults that characterize the same rocks developed at depths deeper than the extensional fractures. Again, by considering the role played by erosion, the faulting represents older events. As a result, we can associate the development of the extensional fractures in the area to the youngest tectonic event/episode that affected the study area.

The computed paleostresses from fault and extensional fracture inversion can be framed into a strike-slip corridor characterized by a poly-phased evolution (Figure 17). Specifically, the left-lateral movement along an E-W trending, regional shear zone would kinematically induce a (crustal) tectonic regime within its deformation region characterized by a NE-SW main horizontal stress and a NW-SE minimum horizontal stress (Figure 17A). Following the geodynamic evolution of the region, influenced by the drifting of the South Atlantic with the associated W and NW movement of the South America plate since Neogene times (Hasui [8]; Cordani et al. [103]; Hasui [104]; Saadi [78]; Torsvik et al. [13]; Richetti et al. [33]; Gomes and Vasconcelos [31]), the strike-slip shear zone was affected by an inversion of the sense of shear. The new right-lateral movement produced the exchange of the previous minimum and maximum horizontal stresses within the regional shear zone being the new maximum horizontal stress NW-SE oriented. This hypothesis is in accordance with the previous studies performed in the study area (e.g., Riccomini [80]; Facincani [79]; Sousa [85]; Morales [66]; Santos and Ladeira [81]; Pinheiro and Queiroz Neto [54]; Pinheiro et al. [67]; Pinheiro and Cianfarra [68]). The younger tectonic setting within the regional shear zone is responsible for the measured systematic and non-systematic joint set trending respectively NW-SE and NE-SW and cutting through the Neocenoic up to Quaternary deposits (Figure 17B). The present day evidences of the older, sinistral tectonic event is mainly represented by the outcropping faults whose main azimuthal family set is nearly parallel with the orientation (around  $N70^\circ E$ , refer to the red Gaussian peak in the fault stereoplot of Figure 17A) of R Riedel faulting associated to an E-W sinistral shear zone. These faults originally formed at low depth and their present near-surface location results from the erosional processes that have been active since their formation age (Paleozoic- or even older- to pre-Neogene times).

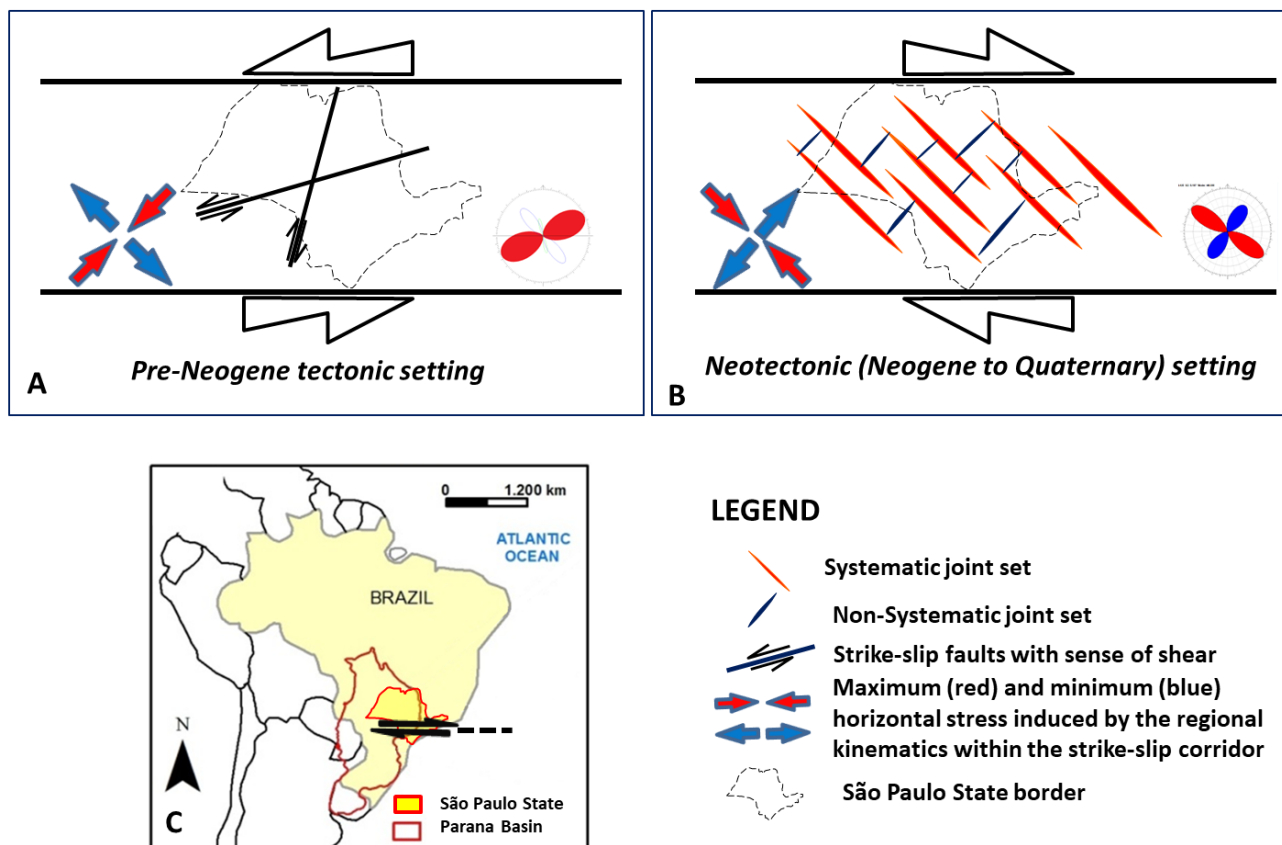


**Figure 17.** Sketch showing the proposed neotectonic evolution of the intraplate strike-slip deformation belt in Southeast Brazil characterized by (A) left-lateral shear followed by (B) right lateral shear. This strike-slip shear zone may represent the onland propagation of oceanic fracture zones (C). Modified from Pinheiro et al. [67].

The proposed strike-slip deformation belt may easily represent the Cenozoic reactivation (Zalán et al. [10]; Cordani et al. [103]; Hasui [8]; Saadi [78]; Vasconcelos et al. [9]; Pinheiro and Cianfarra [68]) of structural trends and weakness zones that played an important role during the Neoproterozoic craton accretion (e.g., Tankard et al. [105]; Almeida et al. [11]; Tello Sáenz et al. [44]) and Mesozoic fragmentation (Franzese and Spalletti [106]; Vaughan et al. [12]; Torsvik et al. [13]; Richetti et al. [33]; Gomes and Vasconcelos [31]) of the Gondwana supercontinent.

This strike-slip shear zone in intraplate settings, characterized by a poly-phased tectonic history, may represent the on-land propagation of oceanic fracture zone (Figure 18A). A similar setting for the study region was previously hypothesized by Zalán et al. [10] and Saadi [78] based on the near parallelism between the inferred continental strike-slip corridor and the offshore tectonic alignments. More recently, Pinheiro et al. [67] suggested a similar geodynamic scenario based on the results of lineament domain analyses. Our results of the paleostresses derived from inversion of faults and extensional fractures collected within the studied region are valid at the regional/crustal scale and further support the hypotheses advanced by other authors (Zalán et al. [10], Saadi [78], Pinheiro et al. [67]) based on independent analyses of different datasets.

Another consideration that further strengthens the reliability of the onshore propagation of (parallel) oceanic fracture zones: both the Brazilian coastline and the continental-ocean boundary present a dextral offset at the latitude of our study region (22°–23° S, Karner and Driscoll [107]; Moulin et al. [108]; Blauch et al. [109]; Magalhães et al. [110]; Figure 18A). At this latitude, the Rio de Janeiro fracture Zone with its associated, sub-parallel fracture swarm is the main tectonic lineament shaping the morphology of the

sea bottom (Granot and Dymant [111]; Pérez-Díaz and Eagles [112]). Seaward, this fracture zone/transform fault marks a dextral offset of the active spreading ridges between South America and Africa, even if they are characterized by sinistral kinematics in their seismically active sections. Similar connections between continental and oceanic tectonic structures have been described in Australia (e.g., Gibson et al. [113]), Africa (Sykes [114]; Antobreh et al. [115]), South America (Mohriak and Rosendahl [116]; Blaich et al. [117]; Vasconcelos et al. [9]), Europe (Barrère et al. [118]); Fazlikhani et al. [119] and Antarctica (Salvini et al. [120]; Storti et al. [121]). Here, the trend of the regional strike-slip fault corridors of the Rennick Geodynamic Belt (e.g., Cianfarra et al. [121]) and of the Matusевич Fault (Flöttmann and Kleinschmidt [122]), coincides with the onland continuation of the offshore Tasman fracture zone (Salvini et al. [120]; Storti et al. [4]; Kleinschmidt and Läufer [123]; Zanutta et al. [124,125]). This fracture zone, similarly to what was described in the South Atlantic, marks a dextral offset of the Australian–Antarctic spreading ridges and its onland continuation corresponds to a dextral offset of the Antarctic continental shelf (Figure 18B). As expected, there is a similar tectonic setting to the north where the onland continuation of the Tasman fracture zone within Australia corresponds to a zone characterized by Quaternary volcanic activity (e.g., Newer Volcanic Province, Southeast Australia, Lesti et al. [126]). A similar tectonic framework may be expected along other fracture zones in the Southern Atlantic, along other fracture zones that propagate in the South America continent, including the Romanche FZ, the Florianopolis FZ and the Agulhas-Falkland FZ (e.g. Torvisk et al. [127]; Granot and Dymant [111], Vasconcelos et al., [9]).

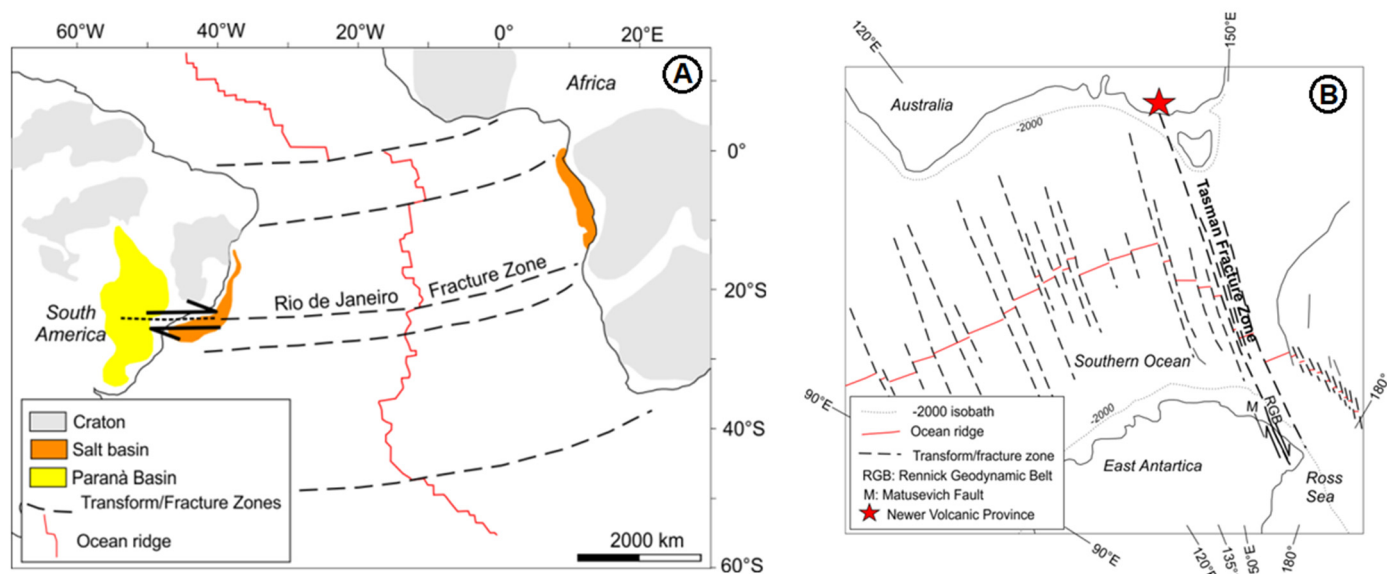


**Figure 18.** Proposed geodynamic model of the on-land propagation of oceanic fracture zone. (A). The intraplate strike-slip corridor affecting the northeastern border of the Parana basin is the continental prosecution of the Rio de Janeiro fracture zone in South Atlantic responsible for the dextral offset of both active spreading ridges and of the Brazilian coastline. Similar geodynamic setting is found in the Southern Ocean. (B). Where the Tasman Fracture Zone propagates both within East Antarctica (with the Rennick Geodynamic Belt, RGB and the Matusевич Fault, M) and in Australia where it is located the Quaternary Newer Volcanic Province (Lesti et al. [126]). Redrawn and modified after Torvisk et al. [127] and Kleinschmidt and Läufer [123].

## 6. Conclusions

The results from the present work allow addressing a series of issue regarding the Cenozoic tectonic evolution of the NE border of the Paraná basin in the framework of regional geodynamics. The adopted original approach of direct inversion by multiple Monte Carlo method allowed identifying the poly-phased tectonic history that affected

the study region. Two paleostress events were computed by fault inversion. The first is characterized by NW-SE minimum horizontal stress and NE-SW maximum horizontal stress in a general extensional regime (sub-vertical  $\sigma_1$ ). The second event is characterized by NW-SE main horizontal stress and NE-SW minimum horizontal stress in a strike-slip tectonic regime (vertical  $\sigma_2$ ). This last stress is compatible with the solution resulting from the extensional fracture inversion characterized by NE-SW minimum horizontal stress and NW-SE maximum horizontal stress. This tectonic setting is confirmed by the result from the inversion of extensional fractures in Quaternary deposits that provides a time constrain for the Neotectonic history of the region.

The computed paleostresses are compatible with the existence of an intraplate strike-slip deformation belt in Southeastern Brazil characterized by an E-W trend. The poly-phased tectonic history of this corridor characterizes an initial left-lateral shear followed by a right-lateral movement whose tectonic activity affected Quaternary deposits also.

The last event correlates to the brittle deformation documented by various authors in Quaternary deposits. In this way, the younger, right-lateral regime is currently affecting the landform evolution of the region, classically interpreted as relics of the old (Paleozoic-Mesozoic) tectonics, produced by lithological variations and/or climatic oscillations.

Finally, we infer that the described intraplate strike-slip deformation belt represents the continental prosecution of the off-shore Rio de Janeiro fracture zones.

The results from this study suggest that it may well be successfully applied along the onshore projection of other fracture zones that populate the Southern Atlantic as well as to other oceans.

The adopted original approach of cumulative inversion of fault and fracture data for (multiple) paleostresses detection revealed successful and results are valid at the regional/crustal scale.

**Author Contributions:** Conceptualization, P.C.; methodology, P.C.; software, F.S.; validation, P.C., M.R.P., F.S. and F.N.J.V.; formal analysis, P.C., M.R.P. and F.S.; investigation, P.C., M.R.P., F.S. and F.N.J.V.; resources, F.N.J.V. and P.C.; data curation, P.C.; writing—original draft preparation, P.C.; writing—review and editing, P.C., M.R.P., F.S. and F.N.J.V.; visualization, P.C. and M.R.P.; supervision, P.C.; project administration, F.N.J.V.; and funding acquisition, F.N.J.V. and P.C. All authors have read and agreed to the published version of the manuscript.

**Funding:** This research was supported by FAPESP, research grant 2016/08722-3 and 2017/14791-0. Part of this research (publication fee) was financially supported by the University of Genova funding to Paola Cianfarra (FRA, Fondi per Ricerca di Ateneo, grant 100022-2020-FRA2019-Cianfarra).

**Informed Consent Statement:** Not applicable.

**Data Availability Statement:** The data presented in this work are available at the Open Science Framework repository (<https://doi.org/10.17605/OSF.IO/VQ5XU>). The analyses were performed by means DAISY3 software (available at <http://host.uniroma3.it/progetti/fralab/Downloads/Programs/> accessed 29 November 2021).

**Acknowledgments:** The authors thank the anonymous reviewers for their thorough reviews that improved the paper. The authors would like to thank: the Nostradamus Research Group (Laboratory of Pedology—Department of Geography—University of São Paulo—Brazil) and the Geoqute Lab scientific team of the Roma Tre University. Constructive discussions of PC and FS with Matteo Maggi that we warmly thank contributed in unravelling the analysis of complex geological and geodynamic systems at the multiple scales of investigations.

**Conflicts of Interest:** The authors declare no conflict of interest.

## References

1. Morgan, W.J. Rises, trenches, great faults, and crustal blocks. *J. Geophys. Res.* **1962**, *73*, 1959–1982. [[CrossRef](#)]
2. Holdsworth, R.E.; Butler, C.A.; Roberts, A.M. The recognition of reactivation during continental deformation. *J. Geol. Soc.* **1997**, *154*, 73–78. [[CrossRef](#)]
3. Wilson, R.W.; Houseman, G.A.; Buitert, S.J.H.; Mccaffrey, K.J.W.; Doré, A.G. Fifty years of the Wilson Cycle Concept in Plate Tectonics: An Overview. *Geol. Soc. Lond. Spec. Publ.* **2019**, *470*, 7. [[CrossRef](#)]

4. Storti, F.; Holdsworth, R.E.; Salvini, F. Intraplate strike-slip deformation belts. *Geol. Soc. Lond. Spec. Publ.* **2003**, *210*, 1–14. [[CrossRef](#)]
5. Dewey, J.F.; Hempton, M.R.; Kidd, W.S.F.; Saroglu, F.; Sengor, A.M.C. Shortening of continental lithosphere in neotectonics of Eastern Anatolia—A young collision zone. In *Collision Tectonics. Geological Society, London, Special Publications*; Coward, M.P., Ries, A.C., Eds.; The Geological Society: London, UK, 1986; Volume 19, pp. 3–36.
6. Molnar, P. Continental tectonics in the aftermath of plate tectonics. *Nature* **1988**, *335*, 131–137. [[CrossRef](#)]
7. Daly, M.C.; Chorowicz, J.; Fairhead, J.D. Rift basin evolution in Africa: The influence of reactivated steep basement shear zones. In *Inversion Tectonics 44. Geological Society, London, Special Publications*; Cooper, M.A., Williams, C.D., Eds.; The Geological Society: London, UK, 1989; pp. 309–334.
8. Hasui, Y. Neotectônica e Aspectos Fundamentais da Tectônica Ressurgente no Brasil. In *1º. Workshop Sobre Neotectônica e Sedimentação Cenozóica Continental no Sudeste Brasileiro, Belo Horizonte*; Boletim no. 11; Sociedade Brasileira de Geologia: São Paulo, Brazil, 1990; pp. 1–31.
9. Vasconcelos, D.L.; Bezerra, F.H.; Clausen, O.R.; Medeiros, W.E.; de Castro, D.L.; Vital, H.; Barbosa, J.A. Influence of Precambrian shear zones on the formation of oceanic fracture zones along the continental margin of Brazil. *Mar. Pet. Geol.* **2019**, *101*, 322–333. [[CrossRef](#)]
10. Zalán, P.V.; Wolff, S.; Conceição, J.C.; Astolfi, M.A.M.; Vieira, I.S.; Appi, C.T.; Zanotto, O.A. Tectônica e sedimentação da Bacia do Paraná. In *Atas do III Simpósio Sul-Brasileiro de Geologia*; Curitiba, Brazil, 1987; Volume 1, pp. 441–477.
11. Almeida, F.F.M.; Brito Neves, B.B.; Carneiro, C.D.R. The origin and evolution of the South American Platform. *Earth Sci. Rev.* **2000**, *50*, 77–111. [[CrossRef](#)]
12. Vaughan, A.P.; Pankhurst, R.J. Tectonic overview of the West Gondwana margin. *Gondwana Res.* **2008**, *13*, 150–162. [[CrossRef](#)]
13. Torsvik, T.H.; Rouse, S.; Labails, C.; Smethurst, M.A. A new scheme for the opening of the South Atlantic Ocean and the dissection of an Aptian salt basin. *Geophys. J. Int.* **2009**, *177*, 1315–1333. [[CrossRef](#)]
14. Lima, C.; Nascimento, E.; Assumpção, M. Stress orientations in Brazilian sedimentary basins from breakout analysis: Implications for force models in the South American Plate. *Geophys. J. Int.* **1997**, *130*, 112–124. [[CrossRef](#)]
15. Roberts, A.M.; Holdsworth, R.E. Linking onshore and offshore structures: Mesozoic extension in the Scottish Highlands. Linking onshore and offshore structures: Mesozoic extension in the Scottish Highlands. *J. Geol. Soc. Lond.* **1999**, *156*, 1061–1064. [[CrossRef](#)]
16. Bezerra, F.H.R.; Rossetti, D.F.; Oliveira, R.G.; Medeiros, W.E.; Brito Neves, B.B.; Balsamo, F.; Nogueira, F.C.C.; Dantas, E.L.; Filho, C.A.; Góes, A.M. Neotectonic reactivation of shear zones and style and geometry in the continental margin of NE Brazil. *Tectonophysics* **2014**, *614*, 78–90. [[CrossRef](#)]
17. Fulfaro, V.J.; Saad, A.R.; Santos, M.V.; Vianna, R.B. Compartimentação e evolução tectônica da Bacia do Paraná [Tectonic compartmentation and evolution of the Paraná Basin]. *Rev. Bras. Geociências* **1982**, *12*, 233–256.
18. Soares, A.P.; Barcellos, P.E.; Csordas, S.M. Lineamentos em imagens de Landsat e Radar e suas implicações no conhecimento tectônico da Bacia do Paraná. *Simpósio Bras. Sens. Remoto* **1982**, *2*, 143–168.
19. Unternehr, P.; Curie, D.; Olivet, J.L.; Goslin, J.; Beuzart, P. South Atlantic fits and intraplate boundaries in Africa and South America. *Tectonophysics* **1988**, *155*, 169–173. [[CrossRef](#)]
20. Zalán, P.V.; Wolff, S.; Conceição, J.C.; Marques, A.; Astolfi, M.A.M.; Vieira, I.S.; Appi, V.T. Bacia do Paraná. In *Origem e evolução de Bacias Sedimentares*; Petrobras: Rio de Janeiro, Brazil, 1990; pp. 135–164.
21. Eyles, C.H.; Eyles, N.; França, A.B. Glaciation and tectonics in an active intracratonic basin: The Late Palaeozoic Itararé Group, Paraná Basin, Brazil. *Sedimentology* **1993**, *40*, 1–25. [[CrossRef](#)]
22. Milani, E.J.; Melo, J.H.G.; De Souza, P.D.; Fernandes, L.A.; França, A.B. Bacia do Paraná. *B. Geoci. Petrobras Rio Jan.* **2007**, *15*, 265–287.
23. De Almeida, F.F.M. Origem e evolução da plataforma brasileira. *Rio Jan. DNPM/DGM Bol.* **1967**, *241*, 36.
24. Neves, B.B.B.; Cordani, U.G. Tectonic evolution of South America during the Late Proterozoic. *Precambrian Res.* **1991**, *53*, 23–40. [[CrossRef](#)]
25. Campanha, G.A.C.; Neves, B.B.B. Frontal and oblique tectonics in the Brazilian Shield. *Episodes* **2004**, *27*, 255–259. [[CrossRef](#)] [[PubMed](#)]
26. Milani, E.J.; Zalán, P.V. An outline of the geology and petroleum systems of the Paleozoic interior basins of South America. *Episodes* **1999**, *22*, 199–205. [[CrossRef](#)]
27. Caputo, M.V.; Crowell, J.C. Migration of glacial centers across Gondwana during Paleozoic Era. *Geol. Soc. Am. Bull.* **1985**, *96*, 1020–1036. [[CrossRef](#)]
28. Riccomini, C.; Velázquez, V.F.; Gomes, C.B. Tectonic controls of the Mesozoic and Cenozoic alkaline magmatism in central-southeastern Brazilian Platform. *Mesoz. Cenozoic Alkaline Magmat. Braz. Platf.* **2005**, *123*, 31–56.
29. Renne, P.R.; Ernesto, M.; Pacca, I.G.; Coe, R.S.; Glen, J.M.G.; Prevot, M.; Perrin, M. The age of Paraná flood volcanism, rifting of gondwanaland, and the Jurassic-Cretaceous boundary. *Science* **1992**, *258*, 975–979. [[CrossRef](#)] [[PubMed](#)]
30. Peate, D.W. The Parana-Etendeka Province. *Geophys. Monogr. Am. Geophys. Union* **1997**, *100*, 217–245.
31. Gomes, A.S.; Vasconcelos, P.M. Geochronology of the Paraná-Etendeka large igneous province. *Earth Sci. Rev.* **2021**, *220*, 103716. [[CrossRef](#)]
32. Rossetti, L.M.; Hole, M.J.; de Lima, E.F.; Simões, M.S.; Millett, J.M.; Rossetti, M.M. Magmatic evolution of Low-Ti lavas in the southern Paraná-Etendeka Large Igneous Province. *Lithos* **2021**, *400*, 106359. [[CrossRef](#)]

33. Richetti, P.C.; Schmitt, R.S.; Reeves, C. Dividing the South American continent to fit a Gondwana reconstruction: A model based on continental geology. *Tectonophysics* **2018**, *747*, 79–98. [[CrossRef](#)]
34. Rossetti, L.M.; Lima, E.F.; Waichel, B.L.; Hole, M.J.; Simões, M.S.; Scherer, C.M.S. Lithostratigraphy and volcanology of the Serra Geral Group, Paraná-Etendeka Igneous Province in Southern Brazil: Towards a formal stratigraphical framework. *J. Volcanol. Geotherm. Res.* **2018**, *355*, 98–114. [[CrossRef](#)]
35. Erlank, A.J.; Marsh, J.S.; Duncan, A.R.; Miller, R.M.; Hawkesworth, C.J.; Betton, P.J.; Rex, D.C. Geochemistry and petrogenesis of the Etendeka volcanic rocks from SWA/Namibia. In *Special Publication of Geological Society of South Africa*; GSSA: Johannesburg, South Africa, 1984; Volume 13, pp. 195–245.
36. Marzoli, A.; Melluso, L.; Morra, V.; Renne, P.R.; Sgrosso, I.; D'Antonio, M.; Morais, E.A.A.; Ricci, G. Geochronology and Petrology of Cretaceous basaltic magmatism in the Kwanza basin (western Angola) and relationships with the Paraná–Etendeka continental flood basalt province. *J. Geodyn.* **1999**, *28*, 341–356. [[CrossRef](#)]
37. Milani, E.J. Evolução tectono-estratigráfica da Bacia do Paraná e seu relacionamento com a geodinâmica fanerozoica do Gondwana Sul-Occidental. Ph.D. Thesis, Institute of Geosciences, Federal University of Rio Grande do Sul, Porto Alegre, Brazil, 1997.
38. Soares, P.C.; Landim, P.M.B.; Fulfaro, V.J. Tectonic cycles and sedimentary sequences in the Brazilian intracratonic basins. *Geol. Soc. Am. Bull. Boulder* **1978**, *89*, 181–191. [[CrossRef](#)]
39. Cordani, U.G.; Neves, B.B.B.; Filho, A.T. Estudo preliminar de integração do Pré-cambriano com os eventos tectônicos das bacias sedimentares brasileiras (atualização). *Bol. Geocienc. Petrobras* **2009**, *17*, 205–219.
40. Soares, P.C. Tectônica sin-sedimentar cíclica na Bacia do Paraná: Controles. Ph.D. Thesis, Departamento de Geologia, Universidade Federal do Paraná, Curitiba, Brazil, 1992; 148p.
41. Almeida, F.F.M.; Hasui, Y. (Eds.) *O Pré-cambriano do Brasil*; Edgar Blucher Ltd.: São Paulo, Brazil, 1984; p. 378.
42. Almeida, F.F.M.; Melo, M.S. Bacia do Paraná e o vulcanismo mesozoico. In *Mapa Geológico do Estado de São Paulo Escala 1:500000, Texto Explicativo*; Almeida, F.F.M., Hasui, Y., Poncano, W.L., Dantas, A.S.L., Melo, M.S., Bistrichi, C.A., Eds.; Instituto de Pesquisas Tecnológicas (IPT): São Paulo, Brazil, 1981; pp. 46–69.
43. Milani, E.J.; Ramos, V.A. Orogenias paleozóicas no domínio Sul-Occidental do Gondwana e os ciclos de subsidência da Bacia do Paraná. *Rev. Bras. Geol.* **1998**, *28*, 473–484. [[CrossRef](#)]
44. Sáenz, C.A.T.; Hackspacher, P.C.; Neto, J.C.H.; Iunes, P.J.; Guedes, S.O.; Ribeiro, L.F.B.; Paulo, S.R. Recognition of Cretaceous, Paleocene and Neogene tectonic reactivation through apatite fission track analysis in Precambrian areas of Southeast Brazil: Association with the opening of the South Atlantic Ocean. *J. S. Am. Earth Sci.* **2003**, *15*, 765–774. [[CrossRef](#)]
45. Ribeiro, L.F.B.; Hackspacher, P.C.; Ribeiro, M.C.S.; Neto, J.C.H.; Tello, S.C.A.; Iunes, P.J.; Franco, A.O.B.; Godoy, D.F. Thermo-tectonic and fault dynamic analysis of Precambrian basement and tectonic with Paraná Basin. *Radiat. Meas.* **2005**, *39*, 669–673. [[CrossRef](#)]
46. Godoy, D.F.; Hackspacher, P.C.; Guedes, S.; Neto, J.C.H. Reconhecimento da tectônica mesozóicacenozóica na borda leste da Bacia do Paraná através da aplicação de traços de fissão em apatitas no Domo de Pitanga (Sudoeste de Rio Claro, SP). *Geociências* **2006**, *25*, 151–164.
47. Pinheiro, M.R.; de Queiroz Neto, J.P. From the semiarid landscapes of southwestern USA to the wet tropical zone of southeastern Brazil: Reflections on the development of cuervas, pediments, and talus. *Earth Sci. Rev.* **2017**, *172*, 27–42. [[CrossRef](#)]
48. Mizusaki, A.M.P.; Thomaz-Filho, A. O magmatismo pós-paleozóico no Brasil. In *Geologia do Continente Sul-Americano: Evolução da Obra de Fernando Flávio Marques de Almeida*; Mantesso-Neto, V., Bartorelli, A., Carneiro, J.C., Brito-Neves, B.B., Eds.; Beca: São Paulo, Brazil, 2004; pp. 281–292.
49. Peate, D.W.; Hawkesworth, C.J.; Mantovani, M.S.M. Chemical stratigraphy of the Paraná lavas (South America): Classification of magma types and their spatial distribution. *Bull. Volcanol.* **1992**, *55*, 119–139. [[CrossRef](#)]
50. Bryan, S.E.; Peate, I.U.; Peate, D.W.; Self, S.; Jerram, D.A.; Mawby, M.R.; Marsh, J.S.; Miller, J.A. The largest volcanic eruptions on Earth. *Earth Sci. Rev.* **2010**, *102*, 207–229. [[CrossRef](#)]
51. Almeida, F.F.M. Síntese sobre a tectônica da Bacia do Paraná (Tectonic synthesis of the Paraná Basin). In *Simpósio Regional De Geologia*; SRG: Curitiba, Brazil, 1980; Volume 3, pp. 1–20.
52. Ross, J.L.S.; Moroz, I.C. *Mapa Geomorfológico do Estado de São Paulo (Map:1:500,000 Scale)*; Revista de Departamento de Geografia: São Paulo, Brazil, 1996.
53. Caetano-Chang, M.R.; Wu, F.T. Arenitos flúvio-eólicos da porção superior da Formação Pirambóia, na porção centro-leste Paulista (Sandy-fluvial sandstones of the upper sector of the Pirambóia Formation in the western-center region of São Paulo State). *Rev. Bras. Geocienc.* **2006**, *36*, 296–304. [[CrossRef](#)]
54. Pinheiro, M.R.; Neto, J.P.Q. Neotectônica e evolução do relevo da região da Serra de São Pedro e do Baixo Piracicaba–Sudeste do Brasil (Neotectonics and landform development of the São Pedro ridge and lower Piracicaba river region/Southeastern Brazil). *Rev. Bras. Geomorf.* **2015**, *16*, 593–613. [[CrossRef](#)]
55. Pinheiro, M.R.; Neto, J.P.D.Q. Geomorphology of the São Pedro Ridge and lower Piracicaba river region, southeastern Brazil. *J. Maps* **2016**, *12*, 377–386. [[CrossRef](#)]
56. Ab'Saber, A.N. Faculty of Philosophy, Languages and Literature, and Human Sciences (Da Participação das Depressões Periféricas e Superfícies Aplainadas na Compartimentação do Planalto Brasileiro). Habilitation Thesis, University of São Paulo, São Paulo, Brazil, 1965.

57. Ab'Saber, A.N. *Paulista Peripheral Depression: A Sector of the Post-Cretaceous Circumdenudation Regions of the Paraná Basin A Depressão Periférica Paulista: Um Setor das Áreas de Circundenação Pós-Cretácica da Bacia do Paraná*; Boletim do Instituto Geografia/USP: São Paulo, Brazil, 1969; Volume 15, pp. 1–15.
58. Pinheiro, M.R. Estudo morfotectônico da região da Serra de São Pedro e do Baixo Piracicaba/SP. Ph.D. Thesis, Department of Geography, Faculty of Philosophy, Languages and Literature, and Human Sciences, University of São Paulo, São Paulo, Brazil, 2014. [[CrossRef](#)]
59. Pinheiro, M.R.; de Queiroz Neto, J.P. Reflexões sobre a gênese da Serra Geral e da Depressão Periférica Paulista: O exemplo da região da Serra de São Pedro e do Baixo Piracicaba, SP. *Rev. Inst. Geológico* **2014**, *35*, 47–59. [[CrossRef](#)]
60. Etchebere, M.L.D.C.; Saad, A.R.; Fulfaro, V.J. Análise de bacia Aplicada À Prospecção de Água Subterrânea No Planalto Ocidental Paulista, SP. *Geociências* **2007**, *26*, 229–247.
61. Strugale, M.; Rostirolla, S.P.; Mancini, F.; Filho, C.V.P.; Ferreira, F.J.F.; de Freitas, R.C. Structural framework and Mesozoic–Cenozoic evolution of Ponta Grossa Arch, Paraná Basin, southern Brazil. *J. S. Am. Earth Sci.* **2007**, *24*, 203–227. [[CrossRef](#)]
62. Costa, D.F.B.D.; Santos, W.H.D.; Bergamaschi, S.; Pereira, E. Analysis of the geometry of diabase sills of the Serra Geral magmatism, by 2D seismic interpretation, in Guareí region, São Paulo, Paraná basin. *Braz. J. Geol.* **2016**, *46*, 605–615. [[CrossRef](#)]
63. Fries, M.; Filho, W.M.; Dourado, J.C.; Fernandes, M.A. Gravimetric survey and modeling of the basement morphology in the sedimentary thickness characterization, NE portion of Paraná Sedimentary Basin. *Braz. J. Geol.* **2017**, *47*, 249–260. [[CrossRef](#)]
64. Hasui, Y.; Borges, M.S.; Morales, N.; Costa, J.B.S.; Bemerguy, R.L.; Jimenez-Rueda, J.R. Intraplate neotectonics in South-East Brazil. In *International Geological Congress, Abstract Volume*; IUGS: Rio de Janeiro, Brazil, 2000; Volume 31, CD-ROM.
65. Riccomini, C. Considerações sobre a posição estratigráfica e tectonismo deformador da Formação Itaqueri na porção centro-leste do Estado de São Paulo. *Rev. Inst. Geol.* **1997**, *18*, 41–48. [[CrossRef](#)]
66. Morales, N. Neotectônica em ambiente intraplaca: Exemplos da região Sudeste do Brasil. Unpublished Free-Docent Thesis, Institute of Geosciences and Exact Sciences of the São Paulo State University, São Paulo, Brazil, 2005.
67. Pinheiro, M.R.; Cianfarra, P.; Villela, F.N.J.; Salvini, F. Tectonics of the Northeastern border of the Parana Basin (Southeastern Brazil) revealed by lineaments domain analysis. *J. S. Am. Earth Sci.* **2019**, *94*, 102231. [[CrossRef](#)]
68. Pinheiro, M.R.; Cianfarra, P. Brittle Deformation in the Neoproterozoic Basement of Southeast Brazil: Traces of Intraplate Cenozoic Tectonics. *Geosciences* **2021**, *11*, 270. [[CrossRef](#)]
69. Ferreira, F.J.F. Integração de dados aeromagnéticos e geológicos: Configuração e evolução tectônica do Arco de Ponta Grossa. Master's Thesis, Instituto de Geociências, Universidade de São Paulo, São Paulo, Brazil, 1982; 170p. [[CrossRef](#)]
70. IPT–Instituto de Pesquisas Tecnológicas do Estado de São Paulo s.a. *Compartimentação Estrutural e Evolução Tectônica do Estado de São Paulo IPT*; Relatório: São Paulo, Brazil, 1989; 27.394.
71. Milani, E.J.; Kinoshita, E.M.; Araujo, L.M.; Cunha, P.R.C. Bacia do Paraná: Possibilidades petrolíferas na calha central. *Bol. Geocienc. Petrobras* **1990**, *4*, 21–34.
72. Quintas, M.C.L. O Embasamento da Bacia do Paraná: Reconstrução Geofísica de seu Arcabouço. Ph.D. Thesis, Institute of Astronomy, Geophysics a Atmospheric Sciences–University of São Paulo, São Paulo, Brazil, 1995.
73. Saad, A.R. Análise da Produção Técnico-Científica. Unpublished Free-Docent Thesis, Institute of Geosciences and Exact Sciences of the São Paulo State University, São Paulo, Brazil, 1997.
74. Campos, A.F.D.; Rostirolla, S.P.; Bartoszeck, M.K.; Romeiro, M.A.T.; Ferreira, F.J.F.; Chang, H.K. Correlação de dados sísmicos multiescala e integração com arcabouço tectônico regional: Exemplo da área do Domo de Piratininga, SP. *Rev. Bras. Geociências* **2008**, *38*, 18–28. [[CrossRef](#)]
75. Rostirolla, S.P.; Assine, M.L.; Fernandes, L.A.; Artur, P.C. Reativação de Paleolineamentos durante a Evolução da Bacia do Paraná–O Exemplo do Alto Estrutural de Quatiguá. *Rev. Bras. Geociências* **2000**, *30*, 639–648. [[CrossRef](#)]
76. Bjornberg, A.J.S. Contribuição ao estudo do cenozóico paulista: Tectônica e sedimentologia. Ph.D. Thesis, São Carlos School of Engineering–University of São Paulo, São Paulo, Brazil, 1969.
77. Curie, D. Ouverture de l'Atlantique sud et discontinuités intra-plaque: Une nouvelle analyse. Ph.D. Thesis, Université de Bretagne Occidentale, Brest, France, 1984; 192p.
78. Saadi, A. Neotectônica da Plataforma Brasileira: Esboço e interpretação preliminares. *Rev. Geon.* **1993**, *1*, 1–15. [[CrossRef](#)]
79. Facincani, E.M. Morfotectônica da Depressão Periférica Paulista, cuesta basáltica e planalto interior. Regiões de São Carlos, Rio Claro e Piracicaba-SP. Ph.D. Thesis, Institute of Geosciences and Exact Sciences of the São Paulo State University, São Paulo, Brazil, 2000.
80. Riccomini, C. Tectonismo Gerador e Deformador dos Depósitos Sedimentares Pósgondvânicos da Porção Centro-Oriental do Estado de São Paulo e Áreas Vizinhas. Unpublished Free-Docent Thesis, Universidade de São Paulo, São Paulo, Brazil, 1995.
81. Santos, M.; Ladeira, F.S.B. Tectonismo em perfis de alteração na serra da Itaqueri (SP): Análise através de indicadores cinemáticos de Falhas (Tectonics in weathering profiles at Itaqueri ridge (SP): Analysis through kinematics indicators of faults). *UNESP. Geociências* **2006**, *25*, 135–149.
82. Guedes, I.C. Análise Morfotectônica do Planalto Ocidental Paulista para Detecção de Deformações Neotectônicas. Ph.D. Thesis, Institute of Geosciences and Exact Sciences of the São Paulo State University, São Paulo, Brazil, 2014.
83. Guedes, I.C.; Morales, N.; Etchebere, M.L.C.; Saad, A.R. Indicações de deformações neotectônicas na bacia do Rio Pardo-SP através de análises de parâmetros fluviomorfométricos e de imagens SRTM (Indications of neotectonic deformations in the Rio Pardo watershed through analysis of fluvial and morphometric parameters and SRTM data). *Geociências* **2015**, *34*, 364–380.

84. Sousa, M.O.L. Caracterização Estrutural do Domo de Pitanga–SP. 116 f. Master’s Thesis, Instituto de Geociências, Universidade Estadual Paulista, Rio Claro, Brazil, 1998.
85. Sousa, M.O.L. Evolução tectônica dos Altos Estruturais de Pitanga, Artemis, Pau d’Alho e Jibóia- Centro do Estado de São Paulo. Master’s Dissertation, Institute of Geosciences and Exact Sciences of the São Paulo State University, São Paulo, Brazil, 2002.
86. Siqueira, L.F.S. Tectônica deformadora em sinéclises intracratônicas: A origem do Alto Estrutural de Pitanga, Bacia do Paraná, SP. Master’s Dissertation, Institute of Geosciences, University of São Paulo, São Paulo, Brazil, 2011.
87. Fernandes, A.J.; Amaral, G. Cenozoic tectonic events at the border of the Parana Basin, São Paulo, Brazil. *J. S. Am. Earth Sci.* **2002**, *14*, 911–931. [[CrossRef](#)]
88. Hasui, Y.; Haralyi, N.; Costa, J. Megaestruturação pré-cambriana do território brasileiro baseada em dados geofísicos e geológicos. *Geociências* **1993**, *12*, 7–31.
89. Nicol, A.; Walsh, J.J.; Watterson, J.; Bretan, P.G. Three-dimensional geometry and growth of conjugate normal faults. *J. Struct. Geol.* **1995**, *17*, 847–862. [[CrossRef](#)]
90. Fossen, H. *Structural Geology*, 2nd ed.; Cambridge University Press: Cambridge, UK, 2016; 524p, ISBN 9781107057647.
91. Caine, J.S.; Evans, J.P.; Forster, C.B. Fault zone architecture and permeability structure. *Geology* **1996**, *24*, 1025–1028. [[CrossRef](#)]
92. Salvini, F.; Vittori, E. Analisi strutturale della linea Olevano-Antrodoco-Posta (Ancona-Anzio Auct.): Metodologia di studio delle deformazioni fragili e presentazione del tratto meridionale. *Mem. Della Soc. Geol. Ital.* **1982**, *24*, 337–356.
93. Cianfarra, P.; Salvini, F. Quantification of fracturing within fault damage zones affecting Late Proterozoic carbonates in Svalbard. *Rend. Lincei* **2016**, *27*, 229–241. [[CrossRef](#)]
94. Salvini, F.; Billi, A.; Wise, D.U. Strike-slip fault-propagation cleavage in carbonate rocks: The Mattinata fault zone, Southern Apennines. Italy. *J. Struct. Geol.* **1999**, *21*, 1731–1749. [[CrossRef](#)]
95. Wise, D.U.; Vincent, R.J. Rotation axis method for detecting conjugate planes in calcite petrofabric. *Am. J. Sci.* **1965**, *263*, 289–301. [[CrossRef](#)]
96. Caputo, R. Evolution of orthogonal sets of coeval extension joints. *Terra Nova* **1995**, *7*, 479–490. [[CrossRef](#)]
97. Price, N.J.; Cosgrove, J.W. *Analysis of Geological Structures*; Cambridge University Press: Cambridge, UK, 1990.
98. Turcotte, D.L.; Schubert, G. *Geodynamics*, 3rd ed.; Cambridge University Press: Cambridge, UK, 2014; ISBN 978-0-521-18623-0.
99. Gross, M.R. The origin and spacing of cross joints: Examples from the Monterey Formation, Santa Barbara Coastline, California. *J. Struct. Geol.* **1993**, *15*, 737–751. [[CrossRef](#)]
100. Balsamo, F.; Storti, F.; Salvini, F.; Silva, A.T.; Lima, C.C. Structural and petrophysical evolution of extensional fault zones in low-porosity, poorly lithified sandstones of the Barreiras Formation, NE Brazil. *J. Struct. Geol.* **2010**, *32*, 1806–1826. [[CrossRef](#)]
101. Tarantola, A. *Inverse Problem Theory and Methods for Model Parameter Estimation*; Society for Industrial and Applied Mathematics: Philadelphia, PA, USA, 2005.
102. Nur, A.; Ron, H.; Scotti, O. Fault mechanics and the kinematics of block rotations. *Geology* **1986**, *14*, 746–749. [[CrossRef](#)]
103. Cordani, U.G.; Neves, B.B.B.; Fuck, R.A.; Filho, A.T.; Cunha, F.M.B. Estudo preliminar de integração do Pré-Cambriano com os eventos tectônicos das bacias sedimentares brasileiras: Petrobrás, Ciência Técnica Petróleo. *Seção Explor. Petróleo* **1984**, *15*, 70.
104. Hasui, Y. A grande colisão pré-cambriana do sudeste brasileiro e a estruturação regional. *Geociências* **2010**, *29*, 141–169.
105. Tankard, A.J.; Uliana, M.A.; Welsink, H.J.; Ramos, V.A.; Turic, M.; França, A.B.; Milani, E.J.; Neves, B.B.D.B.; Eyles, N.; Skarmeta, J.; et al. *Structural and Tectonic Controls of Basin Evolution in Southwestern Gondwana During the Phanerozoic*; AAPG: Tulsa, OK, USA, 1995.
106. Franzese, J.R.; Spalletti, L.A. Late Triassic–early Jurassic continental extension in southwestern Gondwana: Tectonic segmentation and pre-break-up rifting. *J. S. Am. Earth Sci.* **2001**, *14*, 257–270. [[CrossRef](#)]
107. Karner, G.D.; Driscoll, N.W. Tectonic and stratigraphic development of the West African and eastern Brazilian Margins: Insights from quantitative basin modelling. In *The Oil and Gas Habitats of the South Atlantic 153. Geological Society, London, Special Publications*; Cameron, N.R., Bate, R.H., Clure, V.S., Eds.; The Geological Society: London, UK, 1999; pp. 11–40.
108. Moulin, M.; Aslanian, D.; Unternehr, P. A new starting point for south and equatorial Atlantic Ocean. *Earth Sci. Rev.* **2010**, *98*, 1–37. [[CrossRef](#)]
109. Blauch, O.A.; Faleide, J.I.; Tsikalas, F. Crustal breakup and continent-ocean transition at South Atlantic conjugate margins. *J. Geophys. Res.* **2011**, *116*, 1–38. [[CrossRef](#)]
110. Magalhães, J.R.; Barbosa, J.A.; Oliveira, J.T.C.; Filho, M.F.L. Characterization of the ocean-continent transition in the Paraíba Basin and Natal platform region, NE Brazil. *Rev. Bras. Geofísica* **2014**, *32*, 481–496. [[CrossRef](#)]
111. Granot, R.; Jérôme, D. The cretaceous opening of the South Atlantic Ocean. *Earth Planet. Sci. Lett.* **2015**, *414*, 156–163. [[CrossRef](#)]
112. Pérez-Díaz, L.; Eagles, G. Constraining South Atlantic growth with seafloor spreading data. *Tectonics* **2014**, *33*, 1848–1873. [[CrossRef](#)]
113. Gibson, G.M.; Totterdell, J.M.; White, L.T.; Mitchell, C.H.; Stacey, A.R.; Morse, M.P.; Whitaker, A. Pre-existing basement structure and its influence on continental rifting and fracture zone development along Australia’s southern rifted margin. *J. Geol. Soc. Lond.* **2013**, *170*, 365–377. [[CrossRef](#)]
114. Sykes, L.R. Intraplate seismicity, reactivation of preexisting zones of weakness, alkaline magmatism, and other tectonism postdating continental fragmentation. *Rev. Geophys. Space Phys.* **1978**, *16*, 621–688. [[CrossRef](#)]
115. Antobreh, A.A.; Faleide, J.I.; Tsikalas, F.; Planke, S. Rift–shear architecture and tectonic development of the Ghana margin deduced from multichannel seismic reflection and potential field data. *Mar. Pet. Geol.* **2009**, *26*, 345–368. [[CrossRef](#)]

116. Mohriak, W.U.; Rosendahl, B.R. Transform zones in the South Atlantic rifted continental margins. In *Intraplate Strike-slip Deformation Belts 210*; Storti, F., Holdsworth, R.E., Salvini, F., Eds.; Geological Society, Special Publications: London, UK, 2003; pp. 211–228.
117. Blaich, O.A.; Tsikalas, F.; Faleide, J.I. Northeastern Brazilian margin: Regional tectonic evolution based on integrated analysis of seismic reflection and potential field data and modelling. *Tectonophysics* **2008**, *458*, 51–67. [[CrossRef](#)]
118. Barrère, C.; Ebbing, J.; Gernigon, L. Offshore prolongation of Caledonian structures and basement characterization in the western Barents Sea from geophysical modelling. *Tectonophysics* **2009**, *470*, 71–88. [[CrossRef](#)]
119. Fazlikhani, H.; Fossen, H.; Gawthorpe, R.; Faleide, J.I.; Bell, R.E. Basement structure and its influence on the structural configuration of the northern North Sea rift. *Tectonics* **2017**, *36*, 1151–1177. [[CrossRef](#)]
120. Salvini, F.; Brancolini, G.; Buseti, M.; Storti, F.; Mazzarini, F.; Coren, F. Cenozoic geodynamics of the Ross Sea region, Antarctica: Crustal extension, intraplate strike-slip faulting, and tectonic inheritance. *J. Geophys. Res. Solid Earth* **1997**, *102*, 24669–24696. [[CrossRef](#)]
121. Storti, F.; Salvini, F.; Rossetti, F.; Morgan, J.P. Intraplate termination of transform faulting within the Antarctic continent. *Earth Planet. Sci. Lett.* **2007**, *260*, 115–126. [[CrossRef](#)]
122. Cianfarra, P.; Rossi, C.; Capponi, G.; Crispini, L.; Federico, L.; Salvini, F. The on-land prosecution of the Tasman Fracture Zone: The structural architecture along the deformation zone of the Rennick Geodynamic Belt (North Victoria Land, Antarctica). In *Geophysical Research Abstracts*; European Geosciences Union: Munich, Germany, 2019; Volume 21.
123. Kleinschmidt, G.; Läufer, A.L. The Matusevich Fracture Zone in Oates Land, East Antarctica. In *Antarctica*; Springer: Berlin/Heidelberg, Germany, 2006; pp. 175–180.
124. Zanutta, A.; Negusini, M.; Vittuari, L.; Cianfarra, P.; Salvini, F.; Mancini, F.; Sterzai, P.; Dubbini, M.; Galeandro, A.; Capra, A. Monitoring geodynamic activity in the Victoria Land, East Antarctica: Evidence from GNSS measurements. *J. Geodyn.* **2017**, *110*, 31–42. [[CrossRef](#)]
125. Zanutta, A.; Negusini, M.; Vittuari, L.; Martelli, L.; Cianfarra, P.; Salvini, F.; Mancini, F.; Sterzai, P.; Capra, A. New Geodetic and Gravimetric Maps to Infer Geodynamics of Antarctica with Insights on Victoria Land. *Remote Sens.* **2018**, *10*, 1608. [[CrossRef](#)]
126. Lesti, C.; Giordano, G.; Salvini, F.; Cas, R. Volcano-tectonic setting of the intraplate, Pliocene–Holocene, Newer Volcanic Province (Southeast Australia): Role of crustal fracture zones. *J. Geophys. Res.* **2008**, *113*, B07407. [[CrossRef](#)]
127. Torsvik, T.H.; Paulsen, T.S.; Hughes, N.C.; Myrow, P.M.; Ganerød, M. The Tethyan Himalaya: Palaeogeographical and tectonic constraints from Ordovician palaeomagnetic data. *J. Geol. Soc.* **2009**, *166*, 679–687. [[CrossRef](#)]